PRE-COSTAR
FOS APERTURE TRANSMISSIONS FOR POINT SOURCES
and
SURFACE BRIGHTNESS OF DIFFUSE SOURCES

R. C. Bohlin

FOS Instrument Science Report CAL/FOS-106
93 October

A. KINNEY
SIB

ABSTRACT

The FOS absolute sensitivities are determined by observations of standard stars in the 4.3" acquisition aperture. For estimates of absolute fluxes of point sources that are observed in smaller apertures, the apparent, measured transmission of the smaller aperture relative to the 4.3" aperture is required. The proposal ID 4211 was designed to extend our knowledge of these aperture corrections and to verify the stability of the throughput relative to earlier measurements by propid 3106 in 1991. Despite the lack of a theoretical explanation, the data demonstrate that the aperture corrections depend on the detector and grating and, therefore, differ from the true transmission of the aperture, which is a function of only the aperture size and the PSF at the relevant wavelength.

The formula for computing of the specific intensity of sources of diffuse surface brightness depends on the absolute fractional transmission of the 4.3" aperture for a point source but NOT on the aperture correction for a smaller observation aperture.

1. OBSERVATIONS

In order to compute the relative aperture throughput, the countrate spectrum in the smaller apertures is divided by the countrate spectrum of the same star in the A1(4.3") aperture. All of the mean measured aperture corrections in Table 1 are derived from countrates that are corrected to the optimal (zero) OTA focus position according to step 1 of the prescription of Lindler & Bohlin (1993), which is an improvement on the focus correction used to compute the corresponding throughput ratios that appeared in Table 4 of NBH (1992). The OTA focus was +10 microns on 1991.43 for the propid=3106 blue side data, -4 microns on 1991.96 for the propid=3106 red side data, and -3.5 microns for the propid=4211 measurements on 1992.77. The maximum focus corrections are on 1991.43 for the blue side, where the B2(0.3") correction is .92 for the short wavelength gratings H13 and L15 but is less than 5% for the other gratings. For the larger apertures, the correction from +10 to 0 microns is less than 3%, so that errors in the correction procedure cannot cause anomalies larger than 1-2%. The data are recorded at three ybase positions perpendicular to the dispersion and verify the photometric precision, despite the ybase positioning errors discovered by Koratkar and Taylor (1993). The values in Table 1 represent the average ratio of the mean spectrum in the designated aperture divided by the mean spectrum in the A1 (4.3") aperture, as discussed in more detail by NBH.

The target acquistion for these data consists of a four stage peakup, where the final stage is in the B2(0.3") aperture on 0.05" centers in order to limit the pointing uncertainty to 0.025" in each axis. There is an additional pointing tweak in the slit on 0.05" centers in the X axis only. During the side switch from blue to red in propid 4211, only the final stage of the peakup was done in the B2(0.3") aperture. Unfortunately, the extent of this raster pattern was insufficient to acount for the uncertainty in the offset between the sides and resulted in a pointing error of about 0.12" (Bohlin 1993). This 0.12" error means that the red side measurements in 4211 for the 0.5" and the 0.3" apertures are spuriously low. The subsequent red slit tweak up corrected the pointing error for the red side slit observations.

2. THEORY

Table 2 summarizes the expected aperture transmission of the four commonly used apertures relative to the A1(4.3") aperture at optimal OTA focus, as derived from the Table 2 of Lindler & Bohlin (1993), who used the TIM software of Burrows & Hasan (1993) to estimate the aberrated PSF at the FOS entrance apertures. The weak wavelength dependence is caused by the change in the modeled PSF with wavelength and is <2% for the B3(1") and slit over the most relevant wavelength range of 1400 to 5000A on the blue side. The B2(0.3") increases by 4%, while a drop of 10% is predicted for B1(0.5") over the same range. Differences of a few % between Table 2 and the relative transmissions of Evans (1993) are indicative of the fidelity of the TIM model PSF's. In order to compare the data with the theory, Table 3 contains the ratios of the measurements of Table 1 to the predictions of Table 2. The lower limits are omitted in Table 3.

3. DISCUSSION AND RECOMMENDATIONS

The aperture corrections are difficult to measure to a 1% accuracy because of gimp (Fitch et al. 1993), pointing errors, OTA "breathing", jitter, and ybase errors. Even though many of the deviations from unity in Table 3 cannot be explained by these difficulties, the statistical significance of the deviations of the data from the predictions seems undeniable. In particular, consider the differences between the red and blue sides for the high dispersion H gratings. For the 14 cases where the same grating is measured on both sides, all of the red side values exceed the blue measurements, except for one case of equal throughput. This difference is not predicted by the theory; and the predicted 10% drop with wavelength for B1 is not observed, i.e. the measurements of Table 1 are nearer to being constant than the ratios to the theory in Table 3. The TIM output images have a strong resemblance to actual PSF's but are known to suffer some serious imperfections, especially for some non-prime HST camera modes such as PC8. The uncertainties in the model PSF's at the FOS entrance apertures are not quantified and cannot be the basis for the recommended final aperture corrections.

The following is a case-by-case discussion for each aperture-grating combination. These recommended aperture corrections are summarized in Table 4.

3.1 High Dispersion

The small scatter in each of the 8 columns of data for the H gratings in Table 1 suggests that an average of each column might reduce the uncertainties further. An exception is H78, which is slightly low in all four cases.

3.1.1 B3(1")

The blue side average is 0.58 with a maximum deviation of 0.02 or 3%, while the red side mean is 0.60 with 0.02 uncertainty. The excluded measurement for H78 is within the 3% uncertainty.

3.1.2 B1(0.5")

The blue side average is 0.41 with a maximum deviation of 0.01 or 2%, while the red side mean is 0.44 with no scatter among the 4 valid entries. A reasonable error estimate might be 3%. The excluded measurement for H78 is within the uncertainty.

3.1.3 B2(0.3")

The blue side average is 0.27 with a maximum deviation of 0.02 or 7%, while the red side mean is 0.31 with 0.01 scatter among the 4 valid entries. The excluded measurement for H78 is 10% lower than the average; and 10% might be a good choice for an uncertainty, since this small aperture is most suseptible to pointing problems and jitter. For precise absolute flux measurements of point sources, a larger aperture should be used.

3.1.4 C2(0.25x2" slit)

The blue side average is 0.39 with a maximum deviation of 0.01 or 3%, while adopting a red side mean of 0.41 with a nominal 5% or 0.02 uncertainty encompasses the H78 measurement.

3.2 Low Dispersion

Because of the extreme difference that approach 20% between the prism and the L15 measurements, one case of the blue B3(1") aperture is investigated in detail. Pointing errors and jitter problems are minimal for this aperture. Only the L15 spectrum in B3 for propid 4211 shows a spread in the three different Y-base countrates as large as 3%. Y-base errors can only cause a loss of signal, so the aperture correction of 0.64 could be a lower limit but is too large already in comparison with the prism value of 0.53 for the same aperture. The other known effect on aperture transmission is OTA "breathing", i.e. short term OTA focus changes, which are observed to deviate from the nominal by 5 microns during an orbit. However, the A1 reference spectra for the prism and L15 were taken only 4 min apart, while the B3 spectra were also separated by a 4 min time interval. A shift in OTA focus of at least 30 microns in 4 min would be required to cause the observed difference in transmission! Therefore, differences in aperture corrections among dispersing elements must be accepted along with the differences between the blue and red sides.

3.2.1 B3(1")

For L15 on the blue side, 0.65 is recommended because of the possible Y-base error for the other measurement of 0.64, while the red side mean for L15 and L65 is 0.67 with 0.01 scatter. There are only single measurements for the prism. These values differ by around 10% from the high dispersion values, so 10% seems like a safe uncertainty estimate.

3.2.2 B1(0.5")

For L15 on the blue side, 0.46 is the value for both entries in Table 1, while .50 is suggested for the red side L15 and L65. There is no valid measurement for the red side prism, so the blue side is scaled up by the typical difference from the blue to the red side. Again, 10% seems like a safe uncertainty estimate.

3.2.3 B2(0.3")

For L15 on the blue side, 0.31 is the smaller of the two entries in Table 1, while 0.35 is the one valid entry for L65. There is no valid measurement for the red side prism, so the blue side is scaled up by the 0.04 difference between red and blue for the gratings. Again, 10% seems like a safe uncertainty estimate.

3.2.4 C2(0.25x2" slit)

The blue side L15 average is 0.43 with a deviation of 0.01 or 3%, while all three L values on the red side are 0.45. Symmetry with respect to high and low dispersion for the B1(0.5") aperture suggests that the prism corrections for the slit might be 0.02 lower than the quoted values from the single measurements, so 0.03 should be a safe error estimate.

4. WAVELENGTH DEPENDENCE WITHIN THE RANGE OF A SINGLE DISPERSER

According to the theoretical predictions, the variation in the aperture correction within the wavelength range covered by a grating is always less than the ~4% for the B1 (0.5") aperture on the blue L15. For the broad coverage of the prisms, the predicted variation with wavelength approaches 10%. NBH (1992) fit straight lines or quadratics to the aperture corrections as a function of wavelength. Table 5 summarizes the slope of the curve in terms of the ratio of the longest wavelength fit point to the first fit point for the quadratic fits. The aperture corrections do not agree with the predicted transmissions, for example the measured slope for the case of B1(0.5")-blue-L15 is 1.03-1.06 in Table 5, while the TIM prediction is ~0.96. Therefore, the question of wavelength dependence must be answered by the data. One of the main purposes of propid 4211 was to check the repeatability of these slopes that were first measured in propid 3106 by NBH. The slopes did repeat for the test cases of H19 and L15 to an accuracy of 6%. Unfortunately, a couple of the more important cases in the B3 aperture for H13 (0.91) and H27 (0.92) on the blue side show more than a 6% deviation from unity and confirm the necessity of aperture correction that vary with wavelength.

A search of the archive revealed one more propid=3235, which again verifies the repeatability of both the aperture correction and the slope for the important cases of B3(1") on the blue side for H13, H19, and H27. In comparison with the adopted value of 0.58 in Table 4, the 3235 data for the aperture corrections are 0.58, 0.58, and 0.57, respectively. All three slopes are within 1% of the values in Table 5! Therefore, the existence of the slopes found by NBH is verified. The aperture corrections are derived from the least square fit of quadratic polynomials as a function of wavelength. For some FOS dispersers that have a rapid drop in sensitivity, separate secondary quadratic fits are required and improve on the single fit reported by NBH. These cases that show a discontinuity in the aperture corrections are caused by the broad aberrated PSF in the 4.3" aperture that results in a slower drop with wavelength in the A1(4.3") aperture than for the smaller apertures. The fits are all shown as the solid line in Figure 1; and the second fit is defined by the three large filled circles. One of the three filled circles always lies at the endpoint of first fit in order to force continuity between the two quadratics. The other two filled circles are the binned averages of the remaining data points. The dashed lines are the adopted average fit, as described in the next paragraph.

The final adopted aperture corrections are the averages of the coefficients from the quadratic fits for the individual measurement sets, where the individual fits are first normalized to the average corrections of Table 4 over the wavelength range of the primary fit. The individual coefficients of the primary fits are written on the plots in Figure 1, while Table 6 contains the applicable wavelength range and number of data sets used to define each set of three average coefficients. The two of the three most discrepant observations in the small B2(0.3") aperture from propid 4211 are excluded from the averaging process for the bad target acquisition on the red side. The H19 and L15 are excluded, while the prism must be used, since 4211 contained the only data available for the prism aperture corrections.

In order for a GO to understand the errors in the pipeline fluxes that are based on the NBH aperture corrections, the following list describes the major changes in order of decreasing numerical effect.

a) Over the small wavelength ranges for the four cases of detector-disperser modes with the secondary fits, the rapid drop in the aperture correction increases the calibrated fluxes by a factor of up to ~5.

b) NBH did not have measurements for the prisms and used the average for the high dispersion gratings. For example, the value for the B3(1.0") aperture should be 0.53 instead of the 0.59 used by NBH for the blue side prism.

c) The biggest difference for the B3(1.0") aperture between NBH and the Table 4 averages is for the high dispersion blue side average of 0.58 and the NBH value of 0.61 for blue H19.

d) A few of the smaller aperture transmission estimates are now ~10% larger than the NBH estimates; and the red side B2 aperture correction for L15 is 0.35 in Table 4, while the spuriously low NBH value of 0.29 was caused by large jitter that carried the star out of the 0.3" aperture for a significant fraction of the integration time.

5. DIFFUSE SOURCES

The above discussion of the relative aperture corrections of small apertures with respect to the 4.3" aperture for point sources is NOT relevant to absolute surface brightness estimates for diffuse sources. In terms of the inverse sensitivity S(4.3) of a point source at zero focus in the FOS 4.3" aperture, the flux of a point source with response C in counts/sec is

$$F = C\ S(4.3)\ /\ A(ap)\ ,$$

where A(ap) is the aperture correction defined by Table 6 for the aperture used to make the observation, where C is corrected to zero focus, and where A(4.3)=1 by definition. The inverse sensitivity S(ap)=S(4.3)/A(ap) is the calibration that actually resides in PODPS and that is distributed on request. The specific surface intensity I of a diffuse source that overfills an aperture with effective solid angle of omega(ap) is

$$I = C\ S(4.3)\ T(4.3)\ /\ \mathrm{omega}(ap)\ ,$$

where the best estimates of the effective solid angle subtended by an aperture is still in Lindler, Bohlin, & Hartig (1985), where C is independent of focus and NOT corrected, and where T(4.3) is the absolute transmission at zero focus of the 4.3" acquisition aperture that is used for the primary calibration observations of the standard stars. T(4.3) cannot be measured directly but is estimated to be ~0.73 by Lindler & Bohlin (1993) and 0.70-0.72 by Evans (1993).

6. FUTURE CALIBRATION CHANGES

Since there is little time left before the HST servicing mission, the new aperture corrections will not be immediately implemented in the PODPS pipeline reduction system. Instead, these new aperture corrections will be implemented along with the full scheme to handle the FOS changes in sensitivity with time that is in preparation by Lindler & Bohlin. Following the deployment of COSTAR, any reprocessing of old pre-COSTAR archival data will have the best estimates for FOS calibration parameters.

In the future, even after installation of the COSTAR optics, every absolute calibration observation should include aperture correction measurements for a couple of gratings in order to better characterize the repeatability of the relative throughput for any aperture that is normally used to make precise flux measurements of point sources. The blue side gratings H13 and H27 that have the biggest slopes in the propid 3106 data would be good choices for repeats in the B3 aperture. Since the aperture corrections are a function of grating and detector, all combinations must be done at least once following COSTAR deployment. Hopefully, these new aperture corrections will be more consistent with our expectations.

Ed Smith read a draft of this paper and provided several comments that improved the clarity and content.

REFERENCES

Bohlin, R. C. 1993, FOS Instrument Science Report CAL/FOS-097.

Burrows, C., & Hasan, H. 1993, Telescope Image Modelling User Manual, Version 7c, Release 25 and updates through Release 28.

Evans, I. N. 1993, FOS Instrument Science Report CAL/FOS-105.

Fitch, J. E., Hartig, G. F., Beaver, E. A., and Hier, R. G. 1993, FOS Instrument Science Report CAL/FOS-098.

Koratkar, A., and Taylor, C. J. 1993, FOS Instrument Science Report CAL/FOS-096.

Lindler, D. J., & Bohlin, R. C. 1993, FOS Instrument Science Report CAL/FOS-102.

Lindler, D., Bohlin, R., & Hartig, G. 1985, FOS Instrument Science Report CAL/FOS-019.

Neill, J. D., Bohlin, R. C., & Hartig, G. 1992, FOS Instrument Science Report CAL/FOS-077 (NBH).

TABLE 1

MEAN APERTURE THROUGHPUT RATIOS

GRAT	BLUE B3(1")	RED B3(1")	BLUE B1(0.5")	RED B1(0.5")	BLUE B2(0.3")	RED B2(0.3")	BLUE C2-SLIT	RED C2-SLIT
H13	0.59	...	0.40	...	0.26	...	0.39	...
H13d	0.58							
H19	0.60	0.60	0.42	0.44	0.26	0.31c	0.39	0.41
H19a	0.57	0.60	0.41	0.40b	0.29	0.21b	0.40	0.42
H19d	0.58							
H27	0.57	0.59	0.42	0.44	0.26	0.32	0.39	0.42
H27d	0.57							
H40	0.57	0.61	0.42	0.44	0.27	0.32	0.38	0.42
H57	...	0.59	...	0.44	...	0.31	...	0.41
H78	...	0.58	...	0.43	...	0.28	...	0.39
L15	0.65	0.67	0.46	0.50	0.31	0.30c	0.42	0.45
L15a	0.64c	0.66	0.46	0.44b	0.32	0.25b	0.44	0.45
L65	...	0.67	...	0.51	...	0.35	...	0.45
PRIa	0.53	0.54	0.37	0.36b	0.26	0.20b	0.37	0.39

a) PROPID=4211. Otherwise PROPID=3106.
b) Bad target acquisition. Use as lower limits.
c) Ystep repeatability worse than 3%. Excess jitter or ybase error.
d) PROPID=3235.

TABLE 2

RELATIVE APERTURE TRANSMISSION FROM TIM THEORY AT OTA NOMINAL FOCUS

GRAT	WL	BLUE B3(1")	RED B3(1")	BLUE B1(0.5")	RED B1(0.5")	BLUE B2(0.3")	RED B2(0.3")	BLUE C2-SLIT	RED C2-SLIT
H13	1400	.618	...	.483	...	.314	...	.427	...
H19	2000	.614	.612	.473	.475	.315	.317	.425	.414
H27	3000	.610	.610	.462	.462	.316	.320	.423	.415
H40	4000	.610	.609	.450	.450	.322	.323	.422	.415
H57	5000	.609	.607	.438	.437	.327	.326	.422	.416
H78	8000	...	.614	...	.437	...	.303	...	.407
L15	2000	.614	.612	.473	.475	.315	.317	.425	.414
L65	5000	.609	.607	.438	.437	.327	.326	.422	.416
PRI	3000	.610	.610	.462	.462	.316	.320	.423	.415

TABLE 3

MEASURED THROUGHPUT RELATIVE TO THEORETICAL VALUE

GRAT	BLUE B3(1")	RED B3(1")	BLUE B1(0.5")	RED B1(0.5")	BLUE B2(0.3")	RED B2(0.3")	BLUE C2-SLIT	RED C2-SLIT
H13	0.95	...	0.83	...	0.83	...	0.91	...
H19	0.98	0.98	0.89	0.93	0.83	0.98	0.92	0.99
H19a	0.93	0.98	0.87	...	0.92	...	0.94	1.01
H27	0.93	0.97	0.91	0.95	0.82	1.00	0.92	1.01
H40	0.93	1.00	0.93	0.98	0.84	0.99	0.90	1.01
H57	...	0.97	...	1.01	...	0.95	...	0.99
H78	...	0.94	...	0.98	...	0.92	...	0.96
L15	1.06	1.09	0.97	1.05	0.98	0.95	0.99	1.09
L15a	1.04	1.08	0.97	...	1.02	...	1.04	1.09
L65	...	1.10	...	1.17	...	1.07	...	1.08
PRIa	0.87	0.89	0.80	...	0.82	...	0.87	0.94

a) PROPID=4211. Otherwise PROPID=3106.

TABLE 4

RECOMMENDED APERTURE CORRECTIONS AND UNCERTAINTIES AT NOMINAL OTA FOCUS

GRAT MODE	BLUE	RED	UNC	BLUE	RED	UNC	BLUE	RED	UNC	BLUE	RED	UNC
	B3(1")			B1(0.5")			B2(0.3")			C2-SLIT		
HIGH	0.58	0.60	.02	0.41	0.44	.02	0.27	0.31	.03	0.39	0.41	.02
LOW	0.65	0.67	.06	0.46	0.50	.04	0.31	0.35	.03	0.43	0.45	.03
PRISM	0.53	0.54	.06	0.37	0.39	.04	0.26	0.30	.03	0.37	0.39	.03

The uncertainties (UNC) do not include the possible contributions of pointing errors, OTA "breathing", jitter, or ybase errors in an arbitrary science observation.

TABLE 5

SLOPES OF APERTURE RATIOS ACROSS EACH SPECTRUM

GRAT	BLUE	RED	BLUE	RED	BLUE	RED	BLUE	RED
	B3(1")		B1(0.5")		B2(0.3")		C2-SLIT	
H13	0.91	0.00	0.89	0.00	1.00	0.00	0.96	0.00
H13c	0.90							
H19	0.98	0.99	1.05	1.06	1.05	1.06	1.06	1.04
H19a	0.96	1.02	1.00	1.04	1.04	1.13b	1.01	1.01
H19c	0.97							
H27	0.92	0.95	0.97	0.97	0.97	0.95	0.98	0.97
H27c	0.93							
H40	0.94	0.97	0.94	0.94	0.96	0.97	0.96	0.97
H57	0.00	1.01	0.00	1.02	0.00	0.93	0.00	0.95
H78	0.00	0.96	0.00	1.01	0.00	0.88	0.00	0.94
L15	0.96	0.89	1.06	0.95	1.17	0.94	1.07	0.97
L15a	0.96	0.94	1.03	0.98	1.11	0.95b	1.08	0.91
L65	0.00	0.98	0.00	1.00	0.00	0.95	0.00	0.95
PRIa	0.98	1.19	1.02	1.05	1.06	1.04	1.04	1.12

a) PROPID=4211. Otherwise PROPID=3106.
b) Bad target acquisition. Do not use for final average polynomial fits.
c) PROPID=3235.

TABLE 6

SUMMARY OF AVERAGE FOS APERTURE COEFICIENTS

DETEC	FGWA	APER	C0	C1	C2	WMIN	WMAX	NAV
BLUE	H13	B-1	7.40123e-01	-3.69668e-04	9.36560e-08	1151.00	1609.00	1
BLUE	H13	B-2	2.43460e-01	3.89984e-05	-1.41963e-08	1151.00	1609.00	1
BLUE	H13	B-3	4.40583e-01	3.33357e-04	-1.66872e-07	1151.00	1610.00	2
BLUE	H13	C-2	3.23279e-01	1.34740e-04	-6.20508e-08	1151.00	1610.00	1
BLUE	H19	B-1	8.82408e-02	3.21723e-04	-7.93770e-08	1567.00	2335.00	2
BLUE	H19	B-2	1.83798e-02	2.45943e-04	-5.92163e-08	1567.00	2335.00	2
BLUE	H19	B-3	2.30025e-01	3.88200e-04	-1.05693e-07	1567.00	2335.00	3
BLUE	H19	C-2	4.79387e-02	3.37304e-04	-8.19981e-08	1567.00	2335.00	2
BLUE	H27	B-1	3.05223e-01	8.90864e-05	-1.82856e-08	2213.00	3308.00	1
BLUE	H27	B-2	1.97932e-01	5.99049e-05	-1.20871e-08	2214.00	3308.00	1
BLUE	H27	B-3	6.38760e-01	-2.25195e-06	-6.79883e-09	2213.00	3308.00	2
BLUE	H27	C-2	3.88393e-01	7.00039e-06	-2.29434e-09	2213.00	3308.00	1
BLUE	H40	B-1	3.27705e-01	5.71995e-05	-9.00812e-09	3229.00	4830.00	1
BLUE	H40	B-2	2.41780e-01	2.16797e-05	-3.59468e-09	3229.00	4830.00	1
BLUE	H40	B-3	7.12372e-01	-4.36912e-05	2.65989e-09	3229.00	4830.00	1
BLUE	H40	C-2	4.21993e-01	-5.51728e-06	-5.91773e-10	3229.00	4830.00	1
BLUE	L15	B-1	4.32666e-01	1.45117e-05	2.19650e-10	1151.00	2523.00	2
BLUE	L15	B-2	1.49524e-01	1.51922e-04	-3.35666e-08	1151.00	2523.00	2
BLUE	L15	B-3	7.01490e-01	-3.88495e-05	5.60088e-09	1151.00	2523.00	2
BLUE	L15	C-2	3.16397e-01	1.05644e-04	-2.27679e-08	1151.00	2523.00	2
BLUE	PRI	B-1	3.22353e-01	3.44178e-05	-5.03978e-09	1498.00	4995.00	1
BLUE	PRI	B-1	-1.21560e+00	8.38476e-04	-1.04393e-07	4993.00	5961.00	1
BLUE	PRI	B-2	2.15567e-01	3.03832e-05	-3.96765e-09	1498.00	4995.00	1
BLUE	PRI	B-2	-4.04202e-01	4.26773e-04	-5.85007e-08	4993.00	5961.00	1
BLUE	PRI	B-3	5.12325e-01	1.49739e-05	-2.81263e-09	1498.00	4995.00	1
BLUE	PRI	B-3	-3.05272e-02	5.52881e-04	-8.87815e-08	4993.00	5961.00	1
BLUE	PRI	C-2	3.21130e-01	3.40020e-05	-4.61383e-09	1498.00	4995.00	1
BLUE	PRI	C-2	-4.03502e+00	1.87340e-03	-1.98278e-07	4993.00	5961.00	1
AMBER	H19	B-1	9.71168e-02	3.27939e-04	-7.71301e-08	1588.00	2316.00	2
AMBER	H19	B-2	7.38173e-03	2.89346e-04	-6.80307e-08	1588.00	2317.00	1
AMBER	H19	B-3	2.57219e-01	3.53731e-04	-9.02272e-08	1588.00	2316.00	2
AMBER	H19	C-2	1.03904e-01	3.02940e-04	-7.40159e-08	1588.00	2316.00	2
AMBER	H27	B-1	2.89623e-01	1.24265e-04	-2.49962e-08	2217.00	3284.00	1
AMBER	H27	B-2	1.55147e-01	1.29845e-04	-2.64168e-08	2217.00	3283.00	1
AMBER	H27	B-3	4.68684e-01	1.25618e-04	-2.79710e-08	2217.00	3284.00	1
AMBER	H27	C-2	2.76376e-01	1.09996e-04	-2.20588e-08	2217.00	3284.00	1
AMBER	H40	B-1	3.68828e-01	5.34220e-05	-8.78792e-09	3226.00	4791.00	1
AMBER	H40	B-2	3.35431e-01	-6.26521e-06	-1.91675e-11	3226.00	4791.00	1
AMBER	H40	B-3	4.46254e-01	9.02458e-05	-1.27862e-08	3229.00	4790.00	1
AMBER	H40	C-2	3.31970e-01	4.88348e-05	-7.23698e-09	3226.00	4788.00	1
AMBER	H57	B-1	9.42854e-02	1.18346e-04	-9.99186e-09	4559.00	6829.00	1
AMBER	H57	B-2	7.82160e-03	1.17688e-04	-1.12031e-08	4559.00	6829.00	1
AMBER	H57	B-3	3.86043e-01	7.25897e-05	-6.07072e-09	4561.00	6831.00	1
AMBER	H57	C-2	2.98603e-01	4.89152e-05	-5.08857e-09	4561.00	6829.00	1
AMBER	H78	B-1	6.35974e-01	-5.54944e-05	3.89157e-09	6260.00	8501.00	1
AMBER	H78	B-2	5.66594e-01	-5.13968e-05	2.23867e-09	6263.00	8501.00	1
AMBER	H78	B-3	6.13518e-01	7.03740e-06	-1.19140e-09	6260.00	8501.00	1
AMBER	H78	C-2	5.68258e-01	-3.24092e-05	1.47605e-09	6263.00	8501.00	1
AMBER	L15	B-1	4.61080e-01	6.36551e-05	-2.16757e-08	1619.00	2444.00	2
AMBER	L15	B-1	-1.16501e+02	1.38912e-01	-4.11667e-05	1568.00	1622.00	2
AMBER	L15	B-2	2.80945e-01	9.48045e-05	-2.96085e-08	1619.00	2441.00	1
AMBER	L15	B-2	-1.86656e+02	2.29110e-01	-7.01678e-05	1568.00	1622.00	1
AMBER	L15	B-3	6.86425e-01	6.20320e-05	-3.42390e-08	1619.00	2444.00	2
AMBER	L15	B-3	-4.64569e+02	5.71654e-01	-1.75590e-04	1568.00	1622.00	2
AMBER	L15	C-2	4.41812e-01	4.65140e-05	-2.07239e-08	1619.00	2444.00	2
AMBER	L15	C-2	-2.42038e+02	2.96294e-01	-9.04966e-05	1568.00	1622.00	2

AMBER	L65	B-1	3.42255e-01	6.08407e-05	-5.67747e-09	3752.00	7077.00 1
AMBER	L65	B-1	-8.79137e+01	4.65463e-02	-6.12597e-06	3538.00	3755.00 1
AMBER	L65	B-2	2.08488e-01	5.94196e-05	-5.96003e-09	3752.00	7077.00 1
AMBER	L65	B-2	-8.24104e+01	4.42530e-02	-5.91574e-06	3538.00	3755.00 1
AMBER	L65	B-3	4.79409e-01	7.78557e-05	-7.63811e-09	3752.00	7077.00 1
AMBER	L65	B-3	-1.15509e+02	6.10988e-02	-8.03209e-06	3538.00	3755.00 1
AMBER	L65	C-2	3.20407e-01	5.68714e-05	-5.89795e-09	3752.00	7077.00 1
AMBER	L65	C-2	-8.30983e+01	4.43141e-02	-5.87591e-06	3538.00	3755.00 1
AMBER	PRI	B-1	3.77070e-01	6.32113e-06	-3.38474e-10	1618.00	7480.00 1
AMBER	PRI	B-1	-1.52755e+00	6.96870e-04	-5.86245e-08	7478.00	8890.00 1
AMBER	PRI	B-2	2.31237e-01	4.06172e-05	-4.24250e-09	1618.00	7480.00 1
AMBER	PRI	B-2	-7.26827e+00	2.04362e-03	-1.37986e-07	7478.00	8890.00 1
AMBER	PRI	B-3	5.61766e-01	-2.11169e-05	4.22438e-09	1618.00	7480.00 1
AMBER	PRI	B-3	-1.13509e+01	3.24538e-03	-2.19561e-07	7478.00	8890.00 1
AMBER	PRI	C-2	3.96385e-01	-7.60294e-06	1.73057e-09	1618.00	7480.00 1
AMBER	PRI	C-2	-6.45283e+00	1.92644e-03	-1.34419e-07	7478.00	8890.00 1

A(ap)=C0+C1*W+C2*W**2, where W is the wavelength in Anstroms.

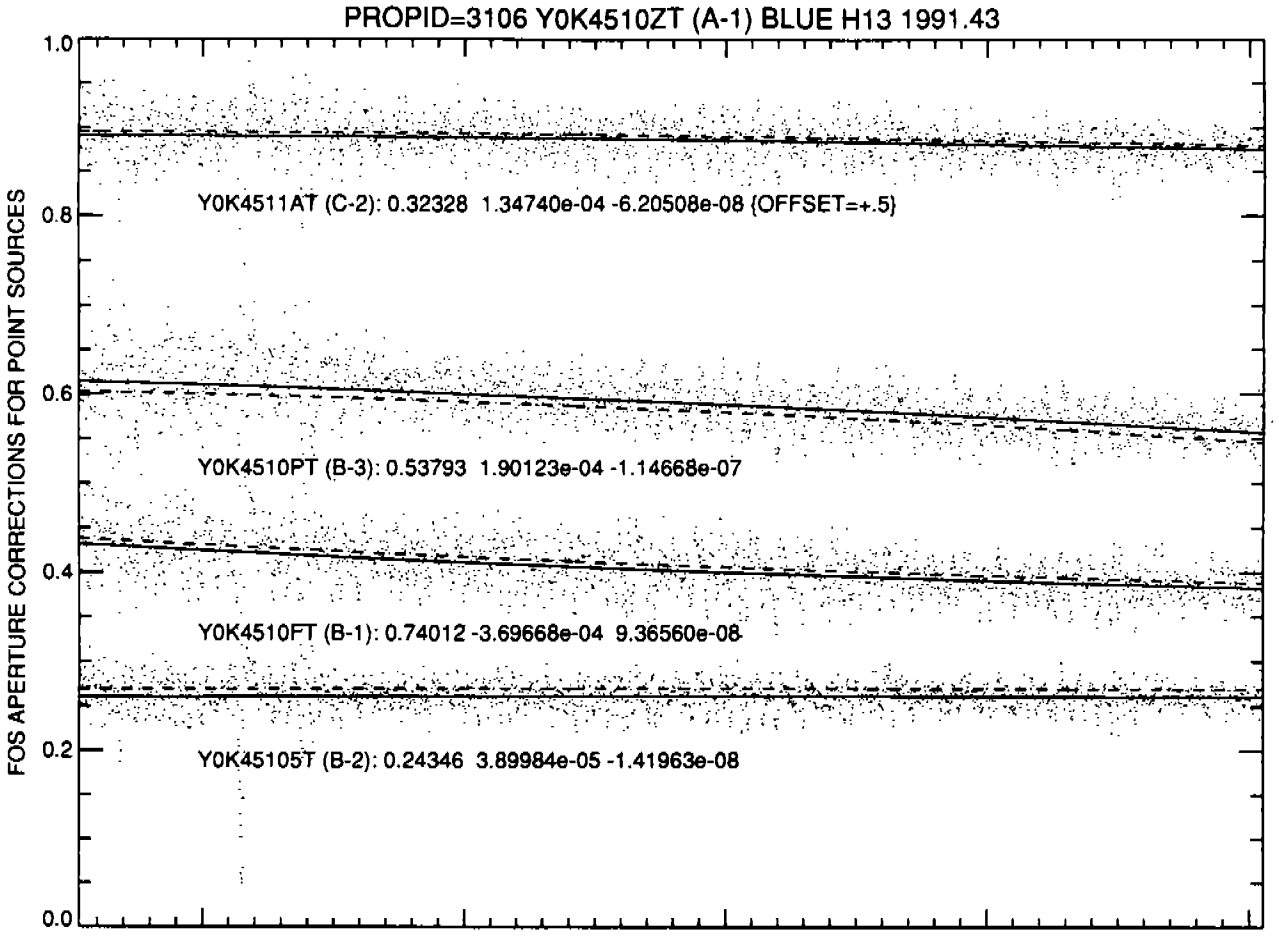
PROPID=3106 Y0K4510ZT (A-1) BLUE H13 1991.43
FOS APERTURE CORRECTIONS FOR POINT SOURCES
1.0
0.8
0.6
0.4
0.2
0.0
Y0K4511AT (C-2): 0.32328 1.34740e-04 -6.20508e-08 (OFFSET=+.5)
Y0K4510PT (B-3): 0.53793 1.90123e-04 -1.14668e-07
Y0K4510FT (B-1): 0.74012 -3.69668e-04 9.36560e-08
Y0K45105T (B-2): 0.24346 3.89984e-05 -1.41963e-08

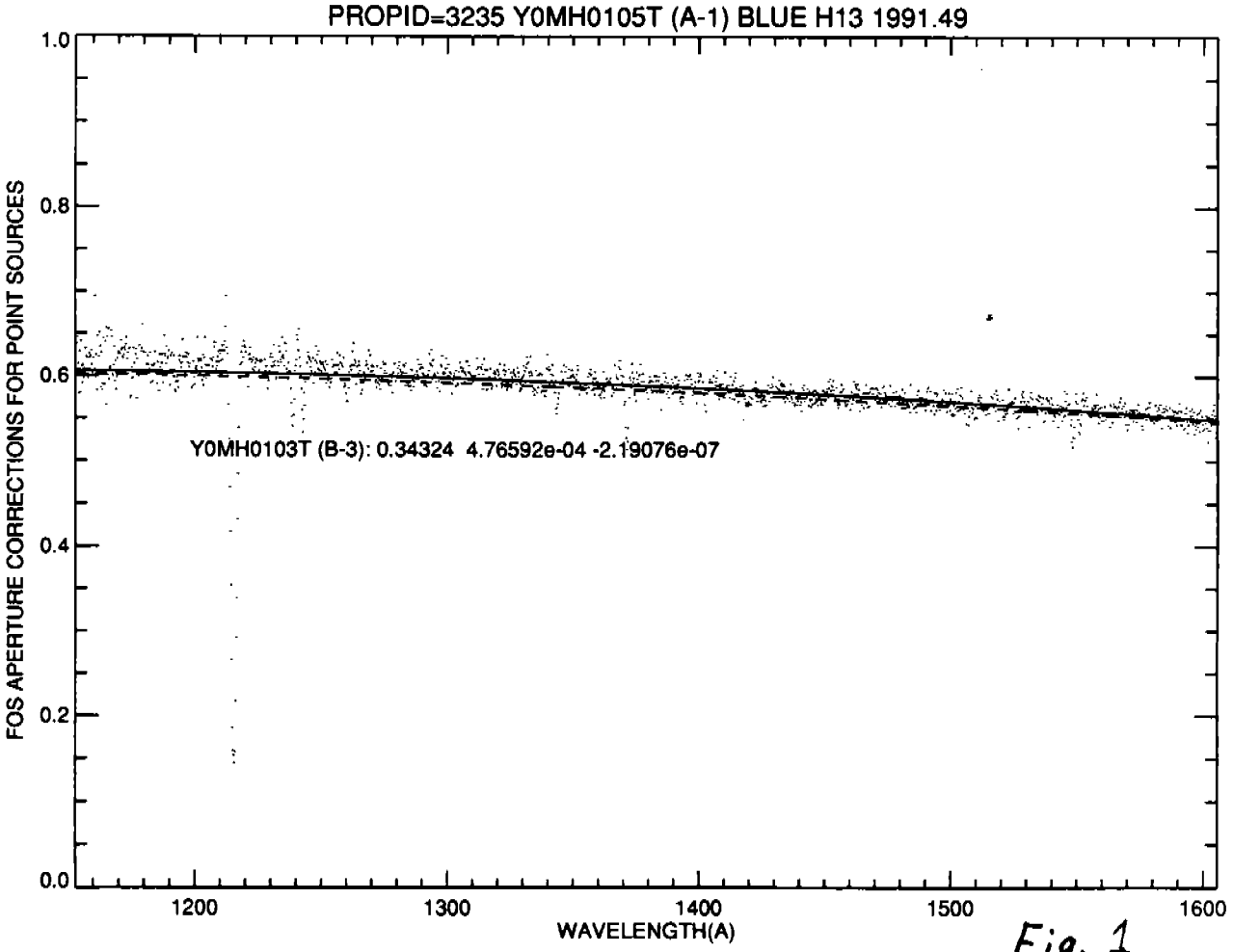
PROPID=3235 Y0MH0105T (A-1) BLUE H13 1991.49
FOS APERTURE CORRECTIONS FOR POINT SOURCES
1.0
0.8
0.6
0.4
0.2
0.0
Y0MH0103T (B-3): 0.34324 4.76592e-04 -2.19076e-07
1200
1300
1400
1500
1600
WAVELENGTH(A)

Fig. 1

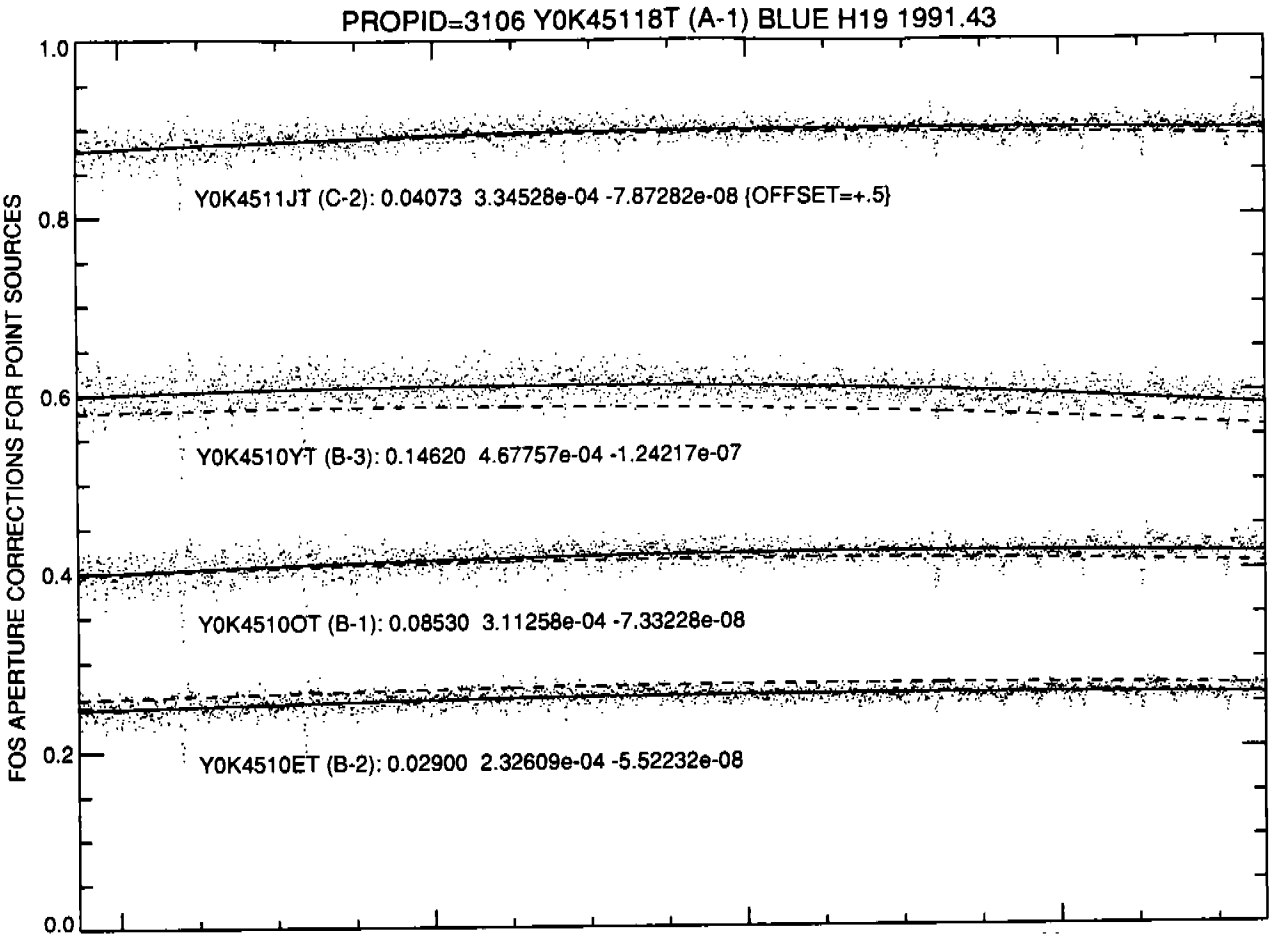
PROPID=3106 Y0K45118T (A-1) BLUE H19 1991.43
FOS APERTURE CORRECTIONS FOR POINT SOURCES
1.0
0.8
0.6
0.4
0.2
0.0
Y0K4511JT (C-2): 0.04073 3.34528e-04 -7.87282e-08 {OFFSET=+.5}
Y0K4510YT (B-3): 0.14620 4.67757e-04 -1.24217e-07
Y0K4510OT (B-1): 0.08530 3.11258e-04 -7.33228e-08
Y0K4510ET (B-2): 0.02900 2.32609e-04 -5.52232e-08

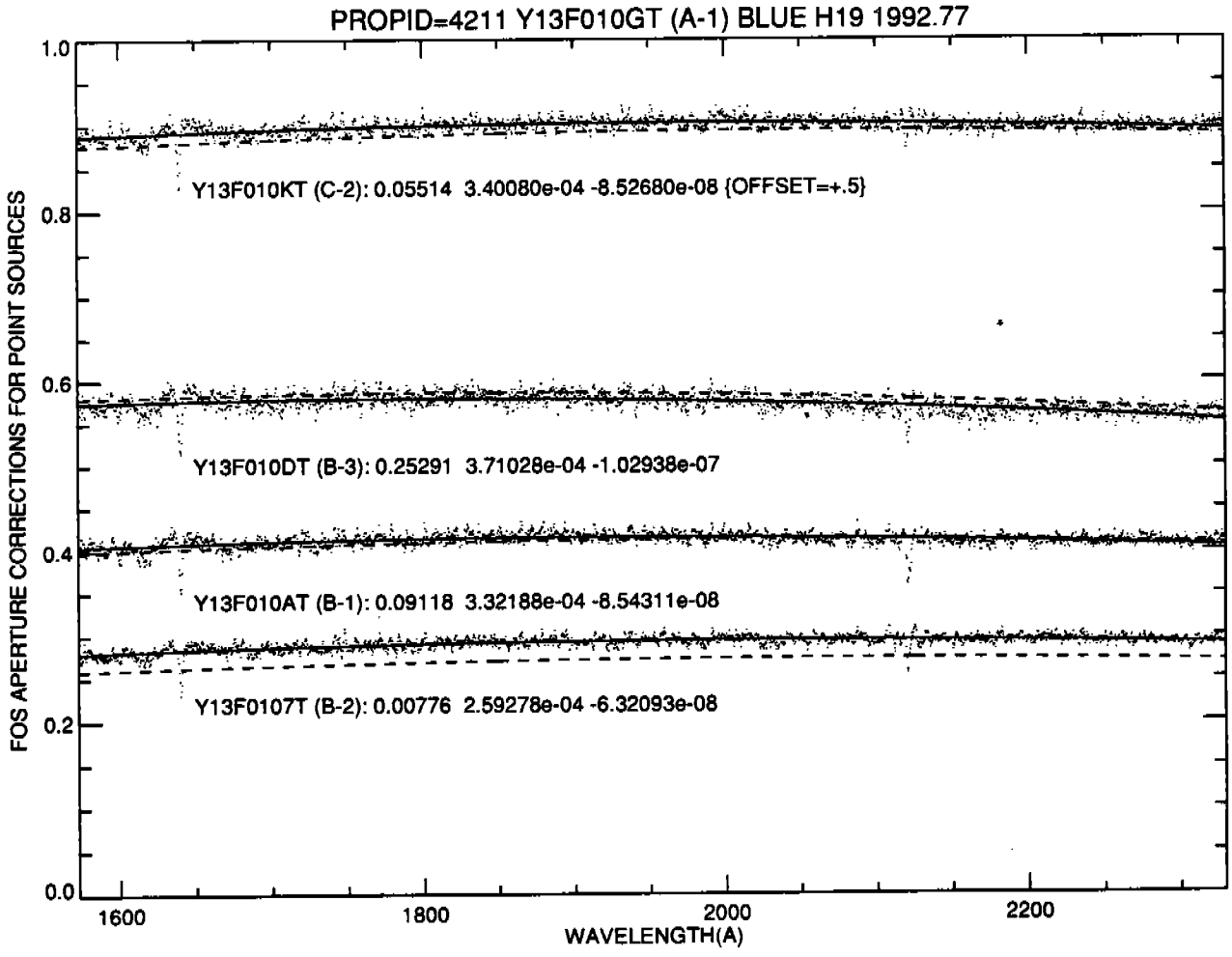
PROPID=4211 Y13F010GT (A-1) BLUE H19 1992.77
FOS APERTURE CORRECTIONS FOR POINT SOURCES
1.0
0.8
0.6
0.4
0.2
0.0
Y13F010KT (C-2): 0.05514 3.40080e-04 -8.52680e-08 {OFFSET=+.5}
Y13F010DT (B-3): 0.25291 3.71028e-04 -1.02938e-07
Y13F010AT (B-1): 0.09118 3.32188e-04 -8.54311e-08
Y13F0107T (B-2): 0.00776 2.59278e-04 -6.32093e-08
1600
1800
2000
2200
WAVELENGTH(A)

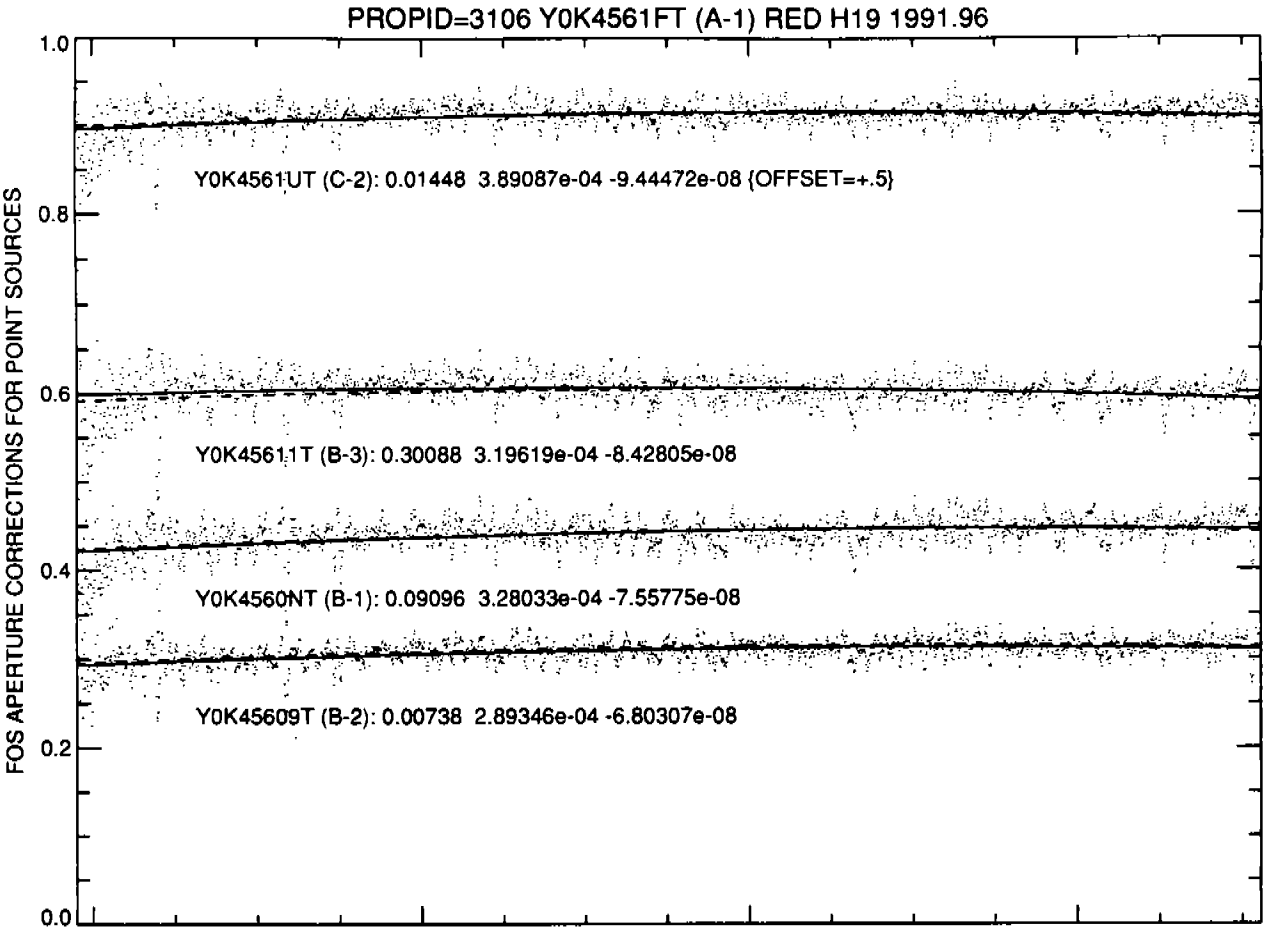
PROPID=3106 Y0K4561FT (A-1) RED H19 1991.96
FOS APERTURE CORRECTIONS FOR POINT SOURCES
1.0
0.8
0.6
0.4
0.2
0.0
Y0K4561UT (C-2): 0.01448 3.89087e-04 -9.44472e-08 {OFFSET=+.5}
Y0K4561:1T (B-3): 0.30088 3.19619e-04 -8.42805e-08
Y0K4560NT (B-1): 0.09096 3.28033e-04 -7.55775e-08
Y0K45609T (B-2): 0.00738 2.89346e-04 -6.80307e-08

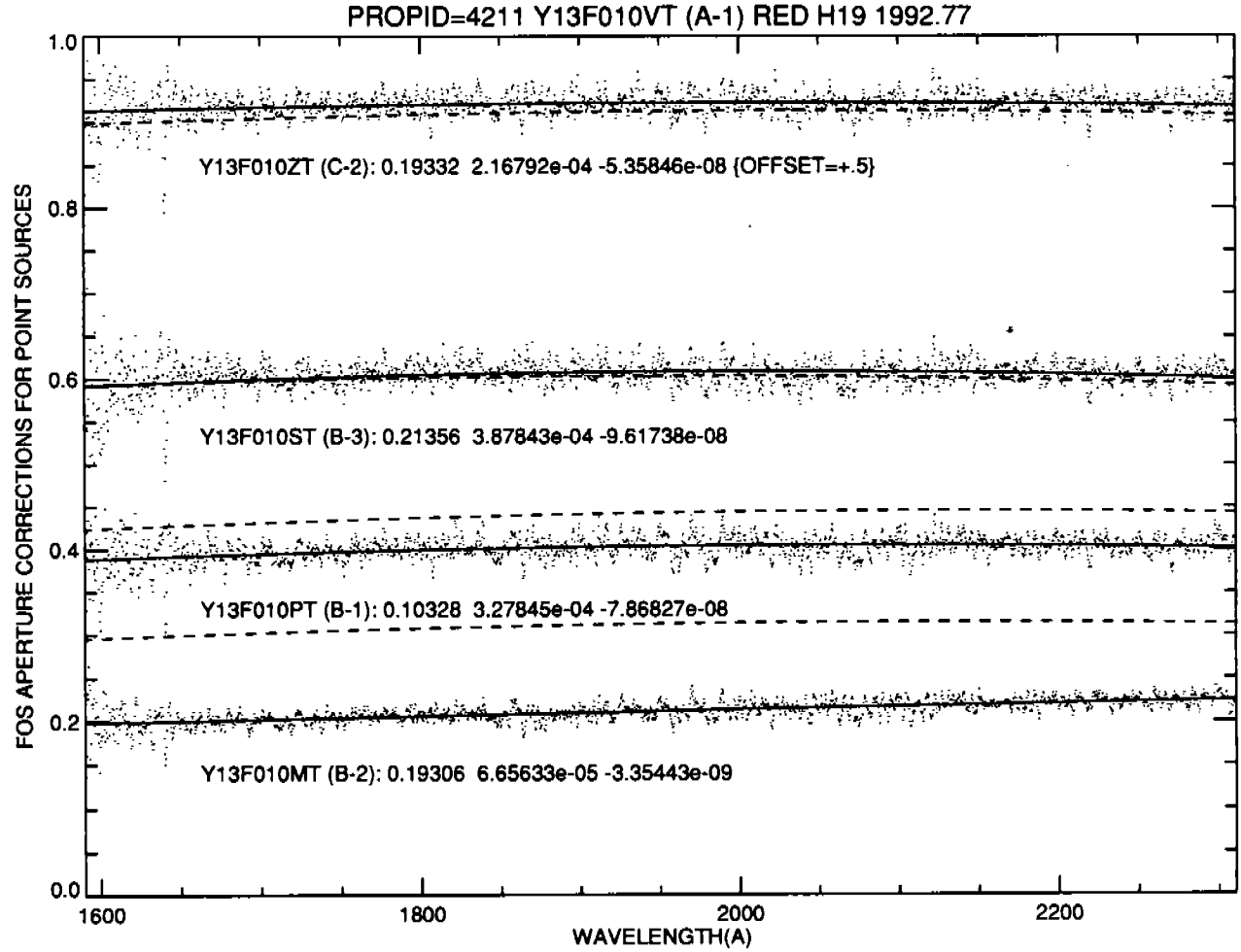
PROPID=4211 Y13F010VT (A-1) RED H19 1992.77
FOS APERTURE CORRECTIONS FOR POINT SOURCES
1.0
0.8
0.6
0.4
0.2
0.0
Y13F010ZT (C-2): 0.19332 2.16792e-04 -5.35846e-08 {OFFSET=+.5}
Y13F010ST (B-3): 0.21356 3.87843e-04 -9.61738e-08
Y13F010PT (B-1): 0.10328 3.27845e-04 -7.86827e-08
Y13F010MT (B-2): 0.19306 6.65633e-05 -3.35443e-09
1600
1800
2000
2200
WAVELENGTH(A)

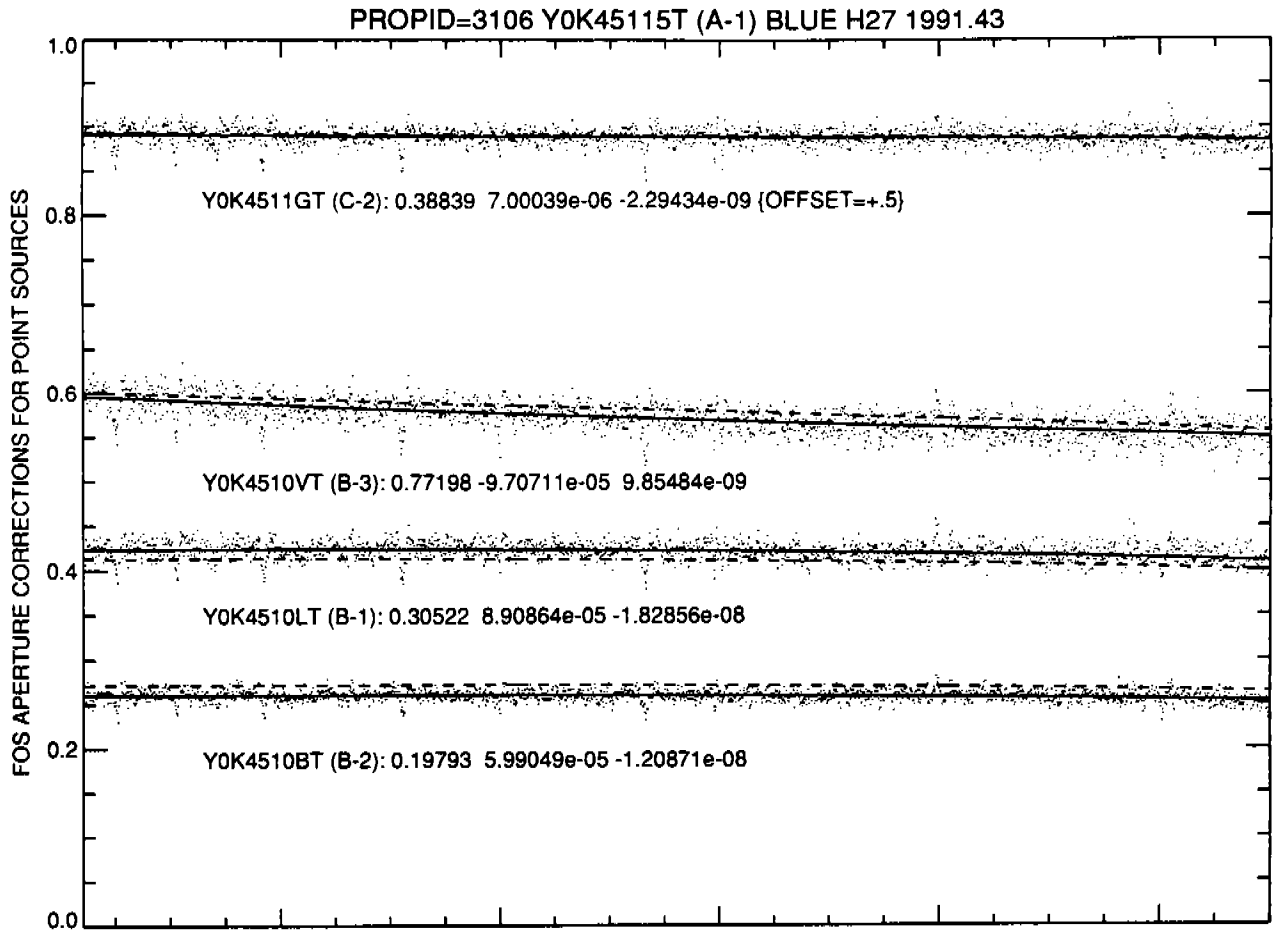
PROPID=3106 Y0K45115T (A-1) BLUE H27 1991.43
FOS APERTURE CORRECTIONS FOR POINT SOURCES
1.0
0.8
0.6
0.4
0.2
0.0
Y0K4511GT (C-2): 0.38839 7.00039e-06 -2.29434e-09 {OFFSET=+.5}
Y0K4510VT (B-3): 0.77198 -9.70711e-05 9.85484e-09
Y0K4510LT (B-1): 0.30522 8.90864e-05 -1.82856e-08
Y0K4510BT (B-2): 0.19793 5.99049e-05 -1.20871e-08

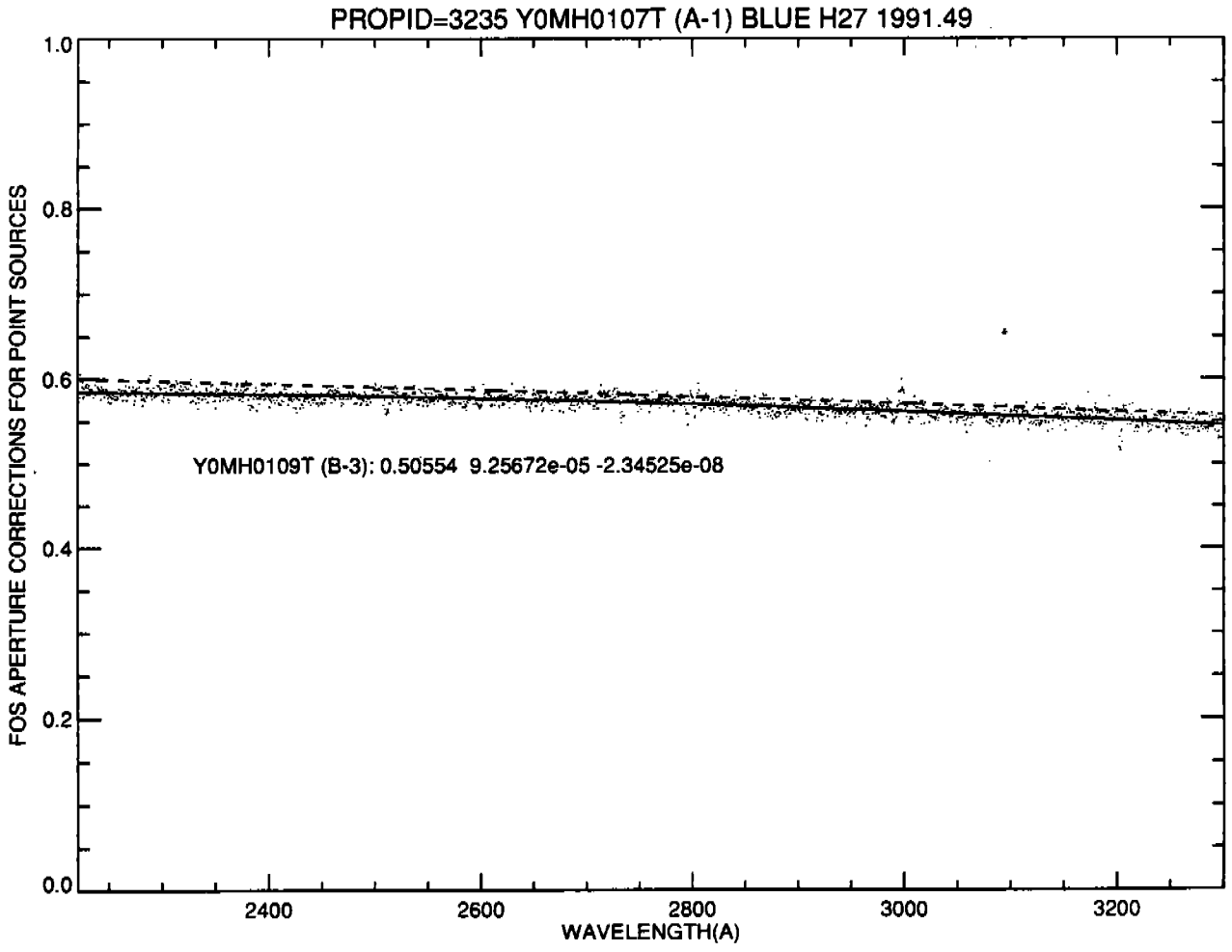
PROPID=3235 Y0MH0107T (A-1) BLUE H27 1991.49
FOS APERTURE CORRECTIONS FOR POINT SOURCES
1.0
0.8
0.6
0.4
0.2
0.0
Y0MH0109T (B-3): 0.50554 9.25672e-05 -2.34525e-08
2400
2600
2800
3000
3200
WAVELENGTH(A)

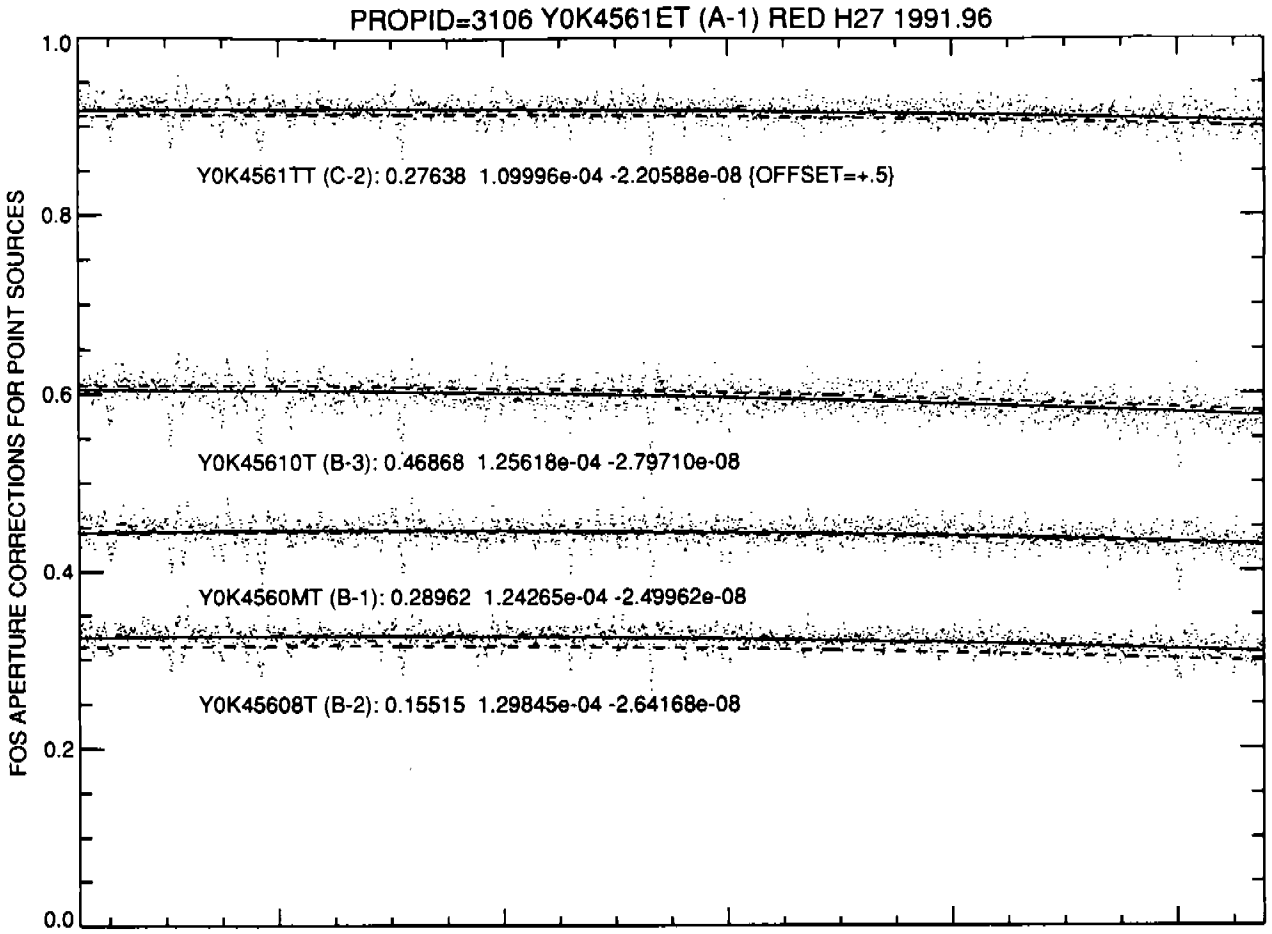
PROPID=3106 Y0K4561ET (A-1) RED H27 1991.96
FOS APERTURE CORRECTIONS FOR POINT SOURCES
1.0
0.8
0.6
0.4
0.2
0.0
Y0K4561TT (C-2): 0.27638 1.09996e-04 -2.20588e-08 {OFFSET=+.5}
Y0K45610T (B-3): 0.46868 1.25618e-04 -2.79710e-08
Y0K4560MT (B-1): 0.28962 1.24265e-04 -2.49962e-08
Y0K45608T (B-2): 0.15515 1.29845e-04 -2.64168e-08

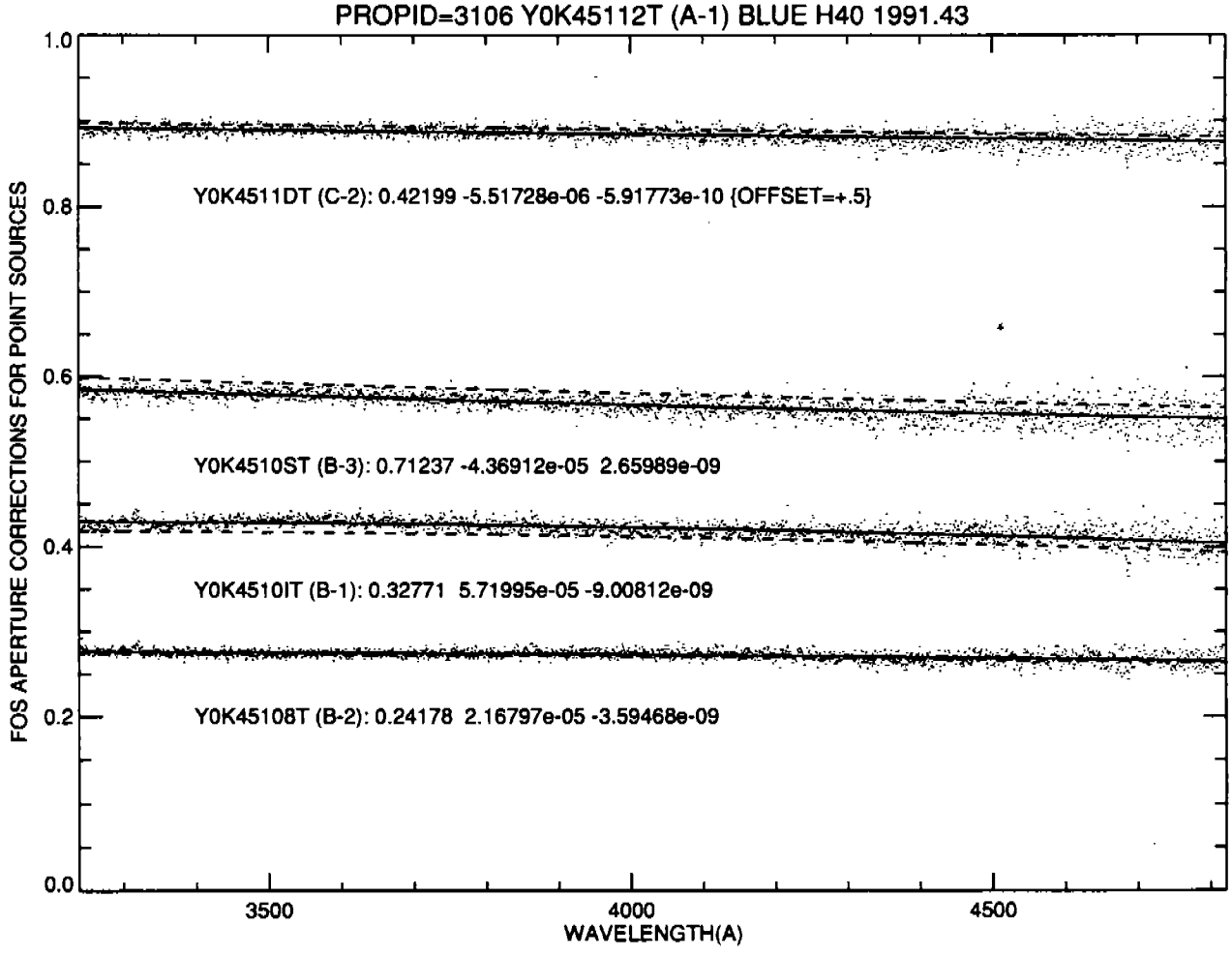
PROPID=3106 Y0K45112T (A-1) BLUE H40 1991.43
FOS APERTURE CORRECTIONS FOR POINT SOURCES
1.0
0.8
0.6
0.4
0.2
0.0
Y0K4511DT (C-2): 0.42199 -5.51728e-06 -5.91773e-10 {OFFSET=+.5}
Y0K4510ST (B-3): 0.71237 -4.36912e-05 2.65989e-09
Y0K4510IT (B-1): 0.32771 5.71995e-05 -9.00812e-09
Y0K45108T (B-2): 0.24178 2.16797e-05 -3.59468e-09
3500
4000
4500
WAVELENGTH(A)

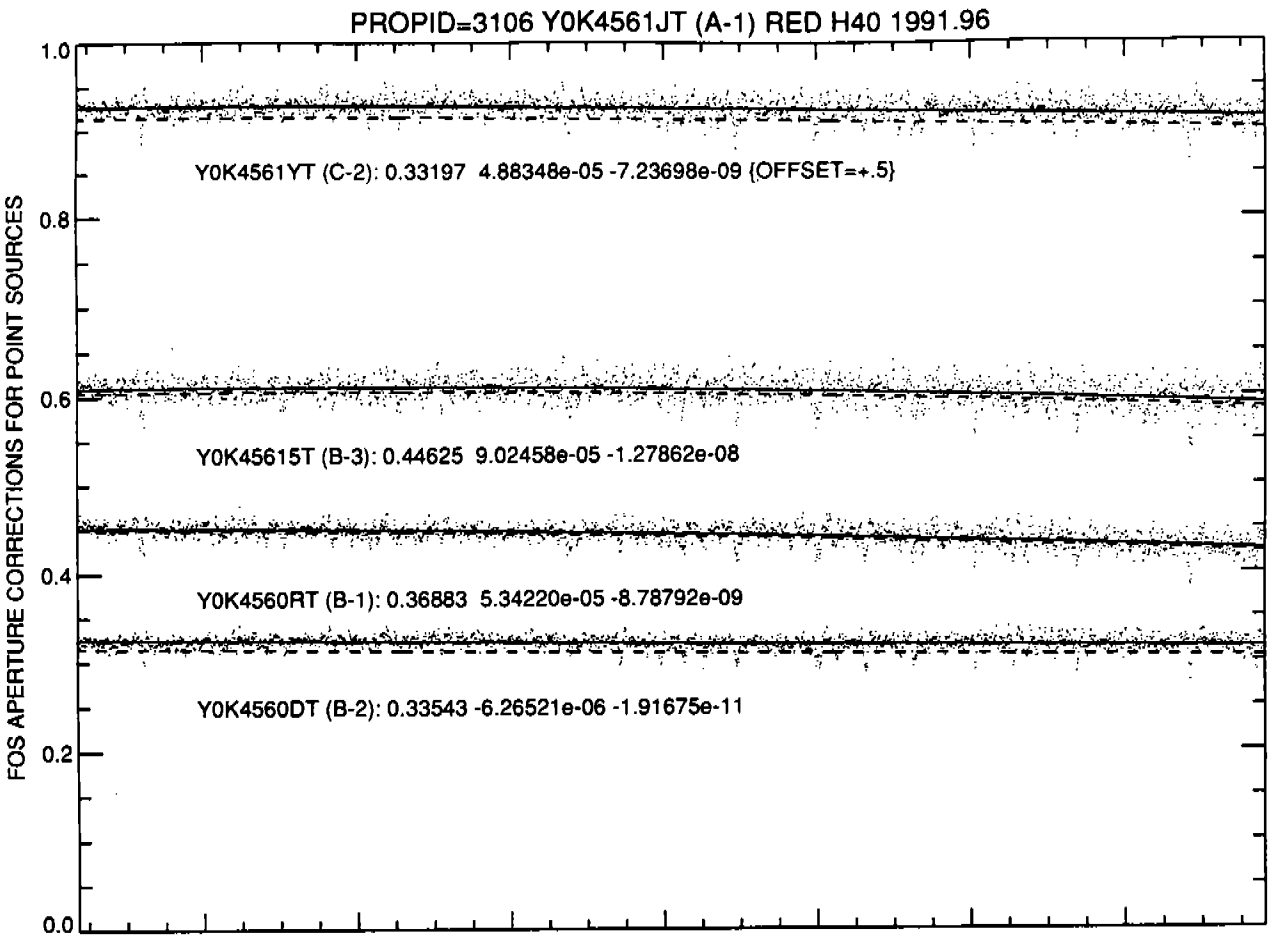
PROPID=3106 Y0K4561JT (A-1) RED H40 1991.96
FOS APERTURE CORRECTIONS FOR POINT SOURCES
1.0
0.8
0.6
0.4
0.2
0.0
Y0K4561YT (C-2): 0.33197 4.88348e-05 -7.23698e-09 {OFFSET=+.5}
Y0K45615T (B-3): 0.44625 9.02458e-05 -1.27862e-08
Y0K4560RT (B-1): 0.36883 5.34220e-05 -8.78792e-09
Y0K4560DT (B-2): 0.33543 -6.26521e-06 -1.91675e-11

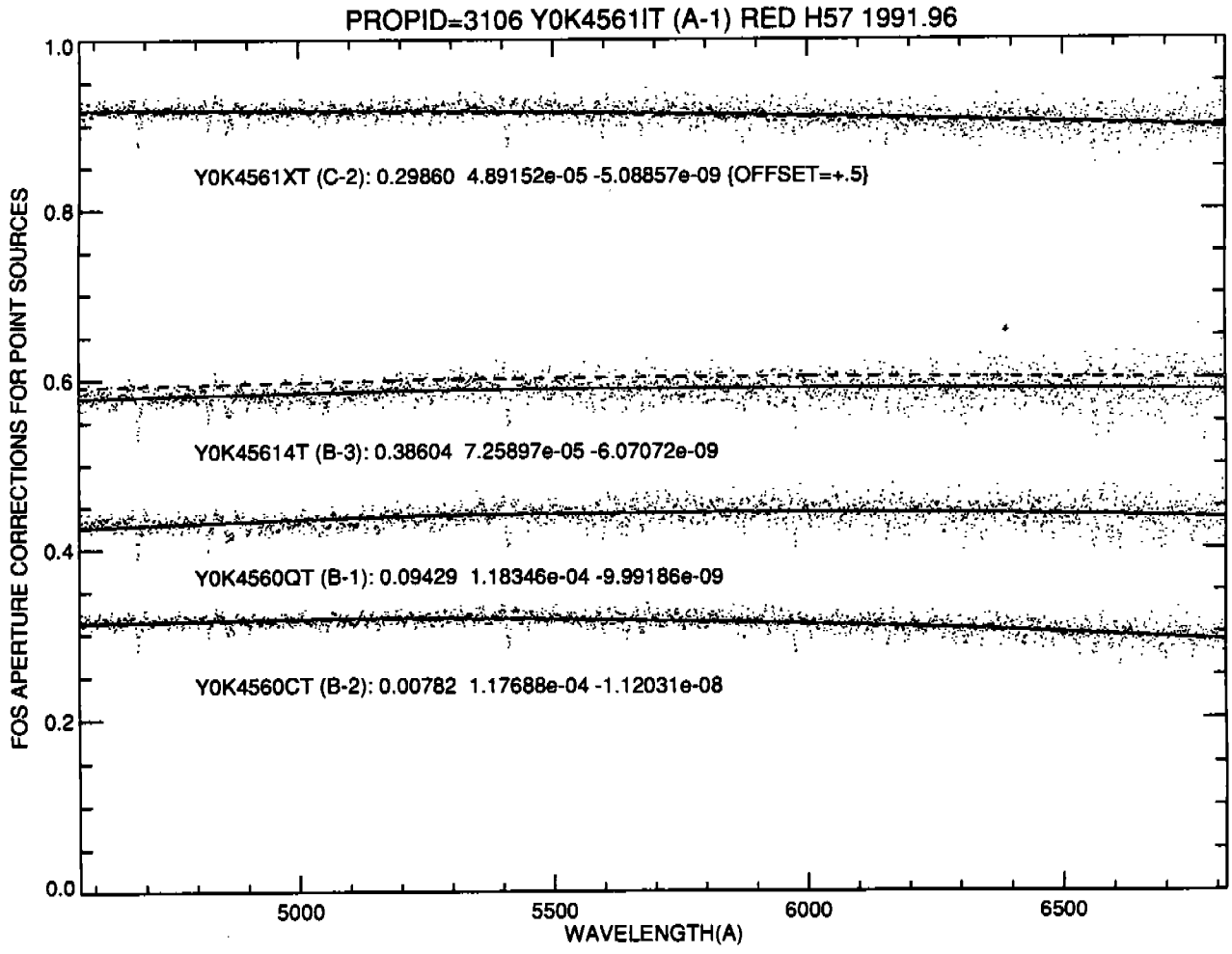
PROPID=3106 Y0K4561IT (A-1) RED H57 1991.96
FOS APERTURE CORRECTIONS FOR POINT SOURCES
1.0
0.8
0.6
0.4
0.2
0.0
Y0K4561XT (C-2): 0.29860 4.89152e-05 -5.08857e-09 {OFFSET=+.5}
Y0K45614T (B-3): 0.38604 7.25897e-05 -6.07072e-09
Y0K4560QT (B-1): 0.09429 1.18346e-04 -9.99186e-09
Y0K4560CT (B-2): 0.00782 1.17688e-04 -1.12031e-08
5000
5500
6000
6500
WAVELENGTH(A)

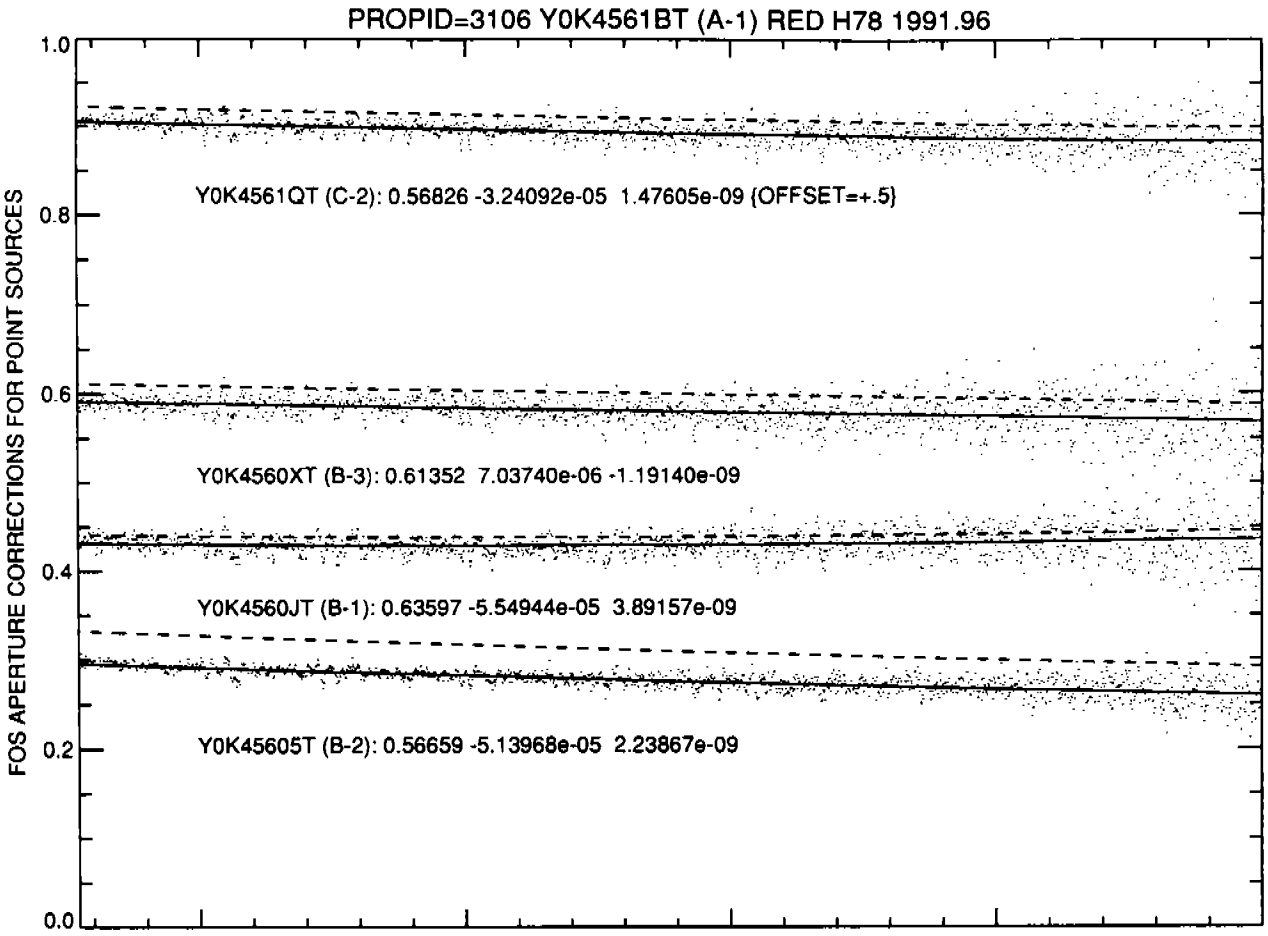
PROPID=3106 Y0K4561BT (A-1) RED H78 1991.96
FOS APERTURE CORRECTIONS FOR POINT SOURCES
1.0
0.8
0.6
0.4
0.2
0.0
Y0K4561QT (C-2): 0.56826 -3.24092e-05 1.47605e-09 {OFFSET=+.5}
Y0K4560XT (B-3): 0.61352 7.03740e-06 -1.19140e-09
Y0K4560JT (B-1): 0.63597 -5.54944e-05 3.89157e-09
Y0K45605T (B-2): 0.56659 -5.13968e-05 2.23867e-09

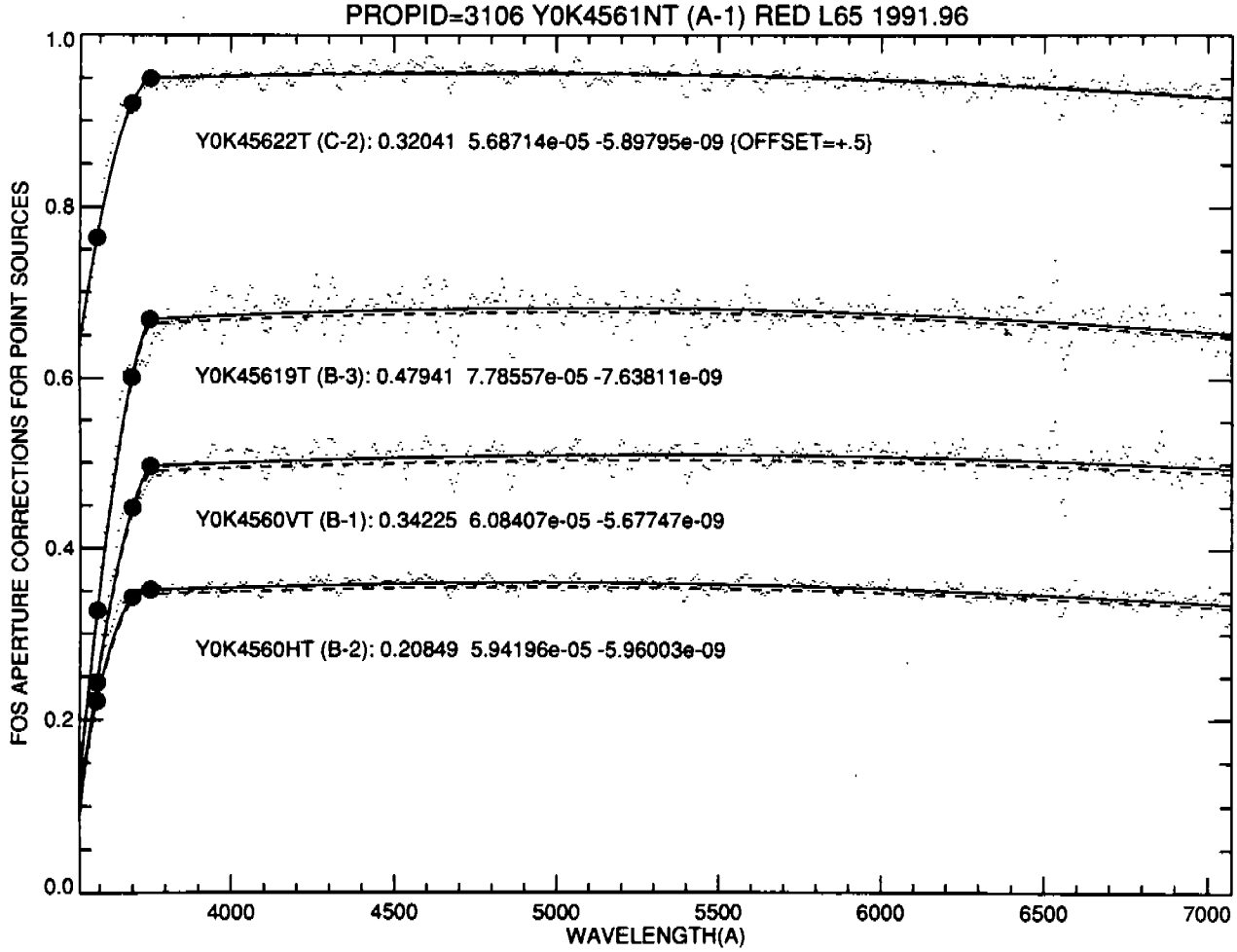
PROPID=3106 Y0K4561NT (A-1) RED L65 1991.96
FOS APERTURE CORRECTIONS FOR POINT SOURCES
1.0
0.8
0.6
0.4
0.2
0.0
Y0K45622T (C-2): 0.32041 5.68714e-05 -5.89795e-09 {OFFSET=+.5}
Y0K45619T (B-3): 0.47941 7.78557e-05 -7.63811e-09
Y0K4560VT (B-1): 0.34225 6.08407e-05 -5.67747e-09
Y0K4560HT (B-2): 0.20849 5.94196e-05 -5.96003e-09
4000
4500
5000
5500
6000
6500
7000
WAVELENGTH(A)

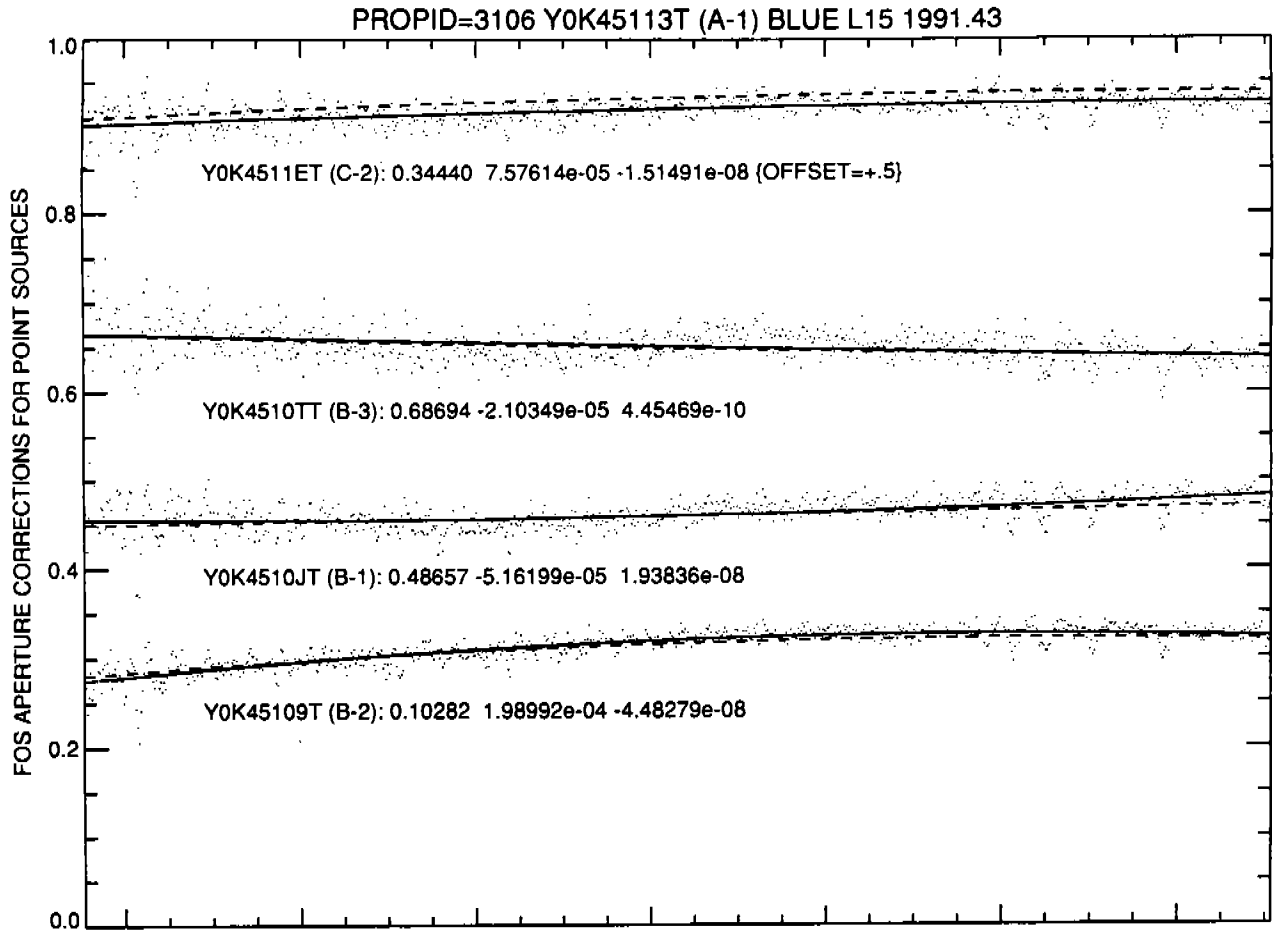
PROPID=3106 Y0K45113T (A-1) BLUE L15 1991.43
FOS APERTURE CORRECTIONS FOR POINT SOURCES
1.0
0.8
0.6
0.4
0.2
0.0
Y0K4511ET (C-2): 0.34440 7.57614e-05 -1.51491e-08 {OFFSET=+.5}
Y0K4510TT (B-3): 0.68694 -2.10349e-05 4.45469e-10
Y0K4510JT (B-1): 0.48657 -5.16199e-05 1.93836e-08
Y0K45109T (B-2): 0.10282 1.98992e-04 -4.48279e-08

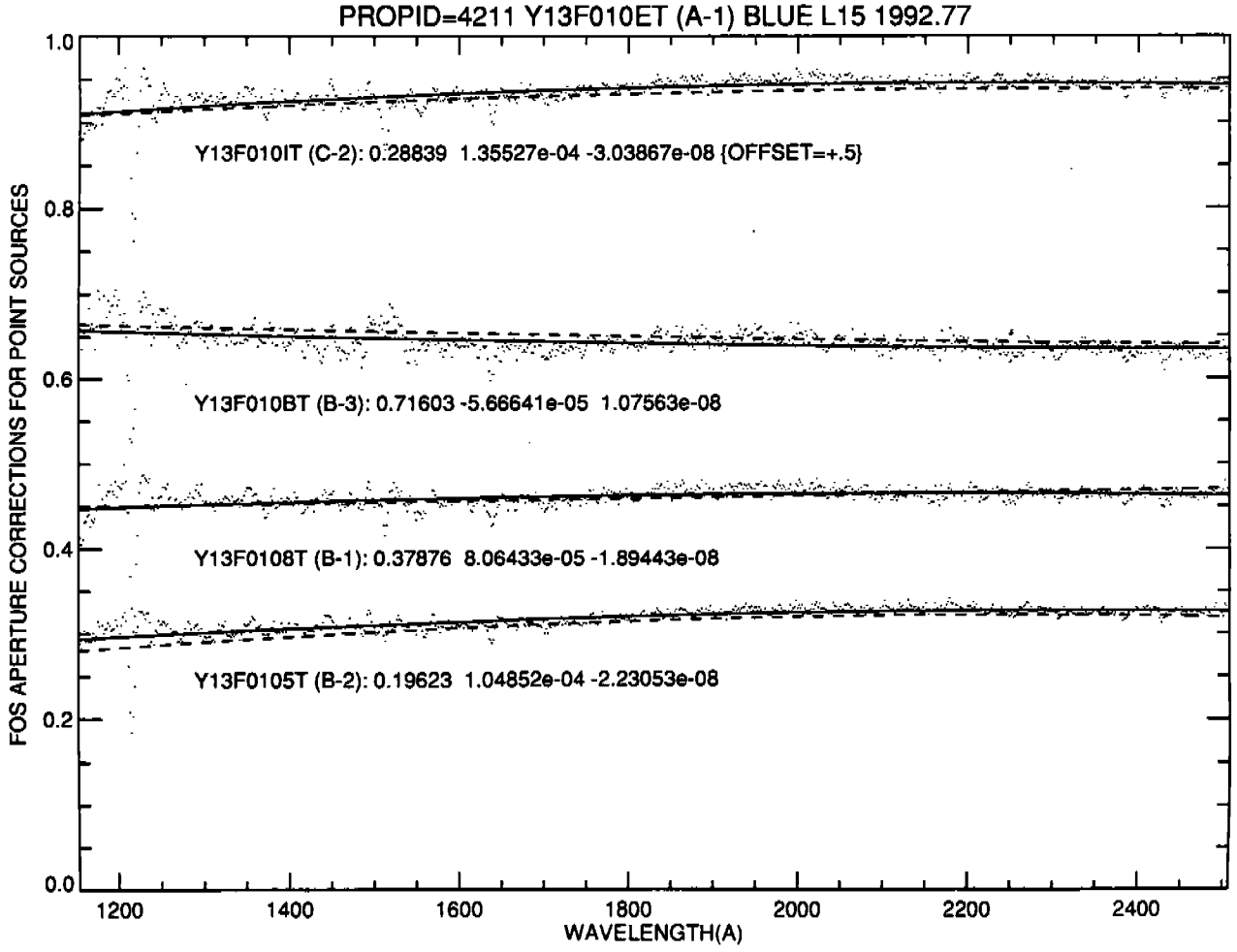
PROPID=4211 Y13F010ET (A-1) BLUE L15 1992.77
FOS APERTURE CORRECTIONS FOR POINT SOURCES
1.0
0.8
0.6
0.4
0.2
0.0
Y13F010IT (C-2): 0.28839 1.35527e-04 -3.03867e-08 {OFFSET=+.5}
Y13F010BT (B-3): 0.71603 -5.66641e-05 1.07563e-08
Y13F0108T (B-1): 0.37876 8.06433e-05 -1.89443e-08
Y13F0105T (B-2): 0.19623 1.04852e-04 -2.23053e-08
1200
1400
1600
1800
2000
2200
2400
WAVELENGTH(A)

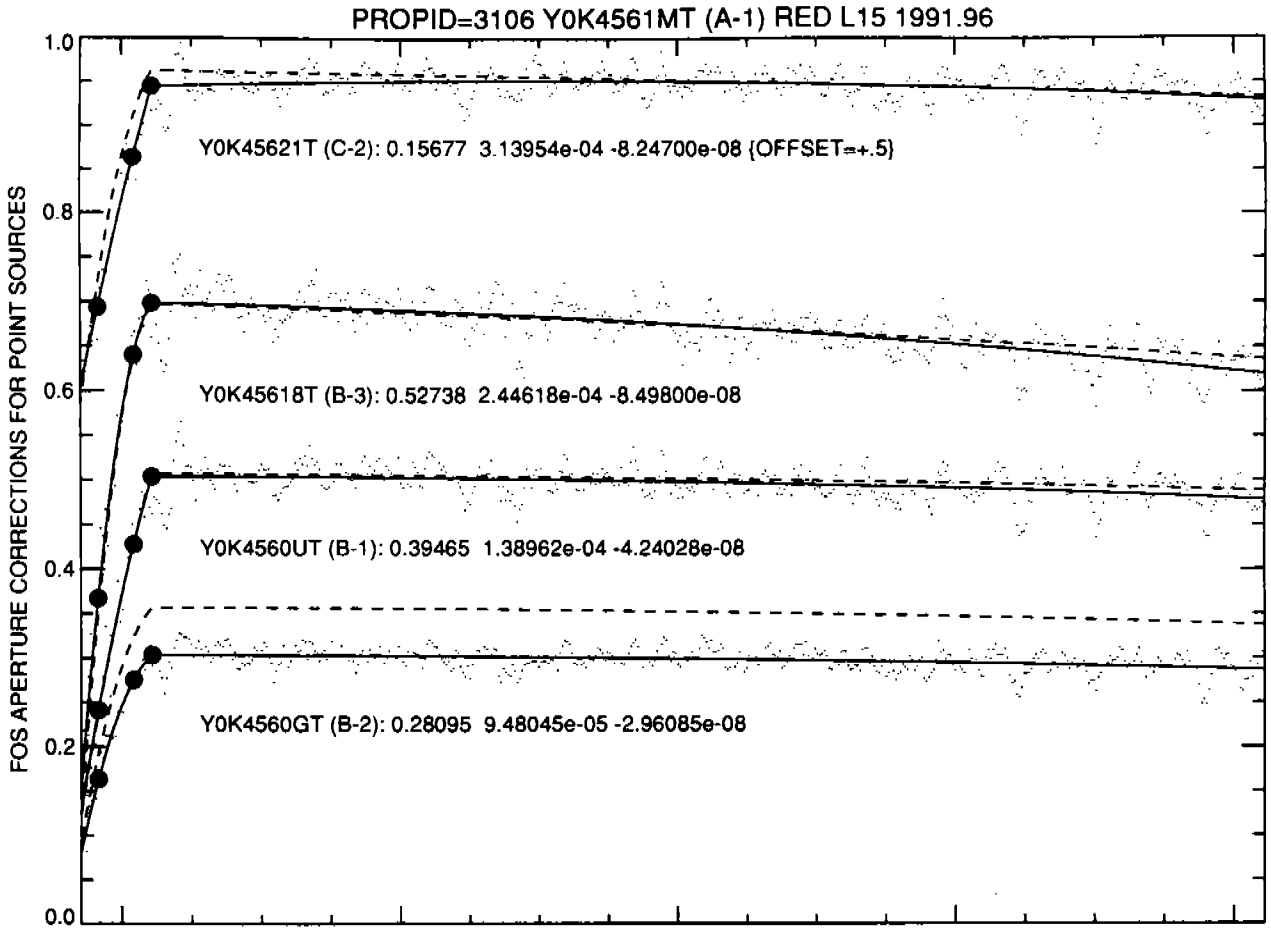
PROPID=3106 Y0K4561MT (A-1) RED L15 1991.96
FOS APERTURE CORRECTIONS FOR POINT SOURCES
1.0
0.8
0.6
0.4
0.2
0.0
Y0K45621T (C-2): 0.15677 3.13954e-04 -8.24700e-08 {OFFSET=+.5}
Y0K45618T (B-3): 0.52738 2.44618e-04 -8.49800e-08
Y0K4560UT (B-1): 0.39465 1.38962e-04 -4.24028e-08
Y0K4560GT (B-2): 0.28095 9.48045e-05 -2.96085e-08

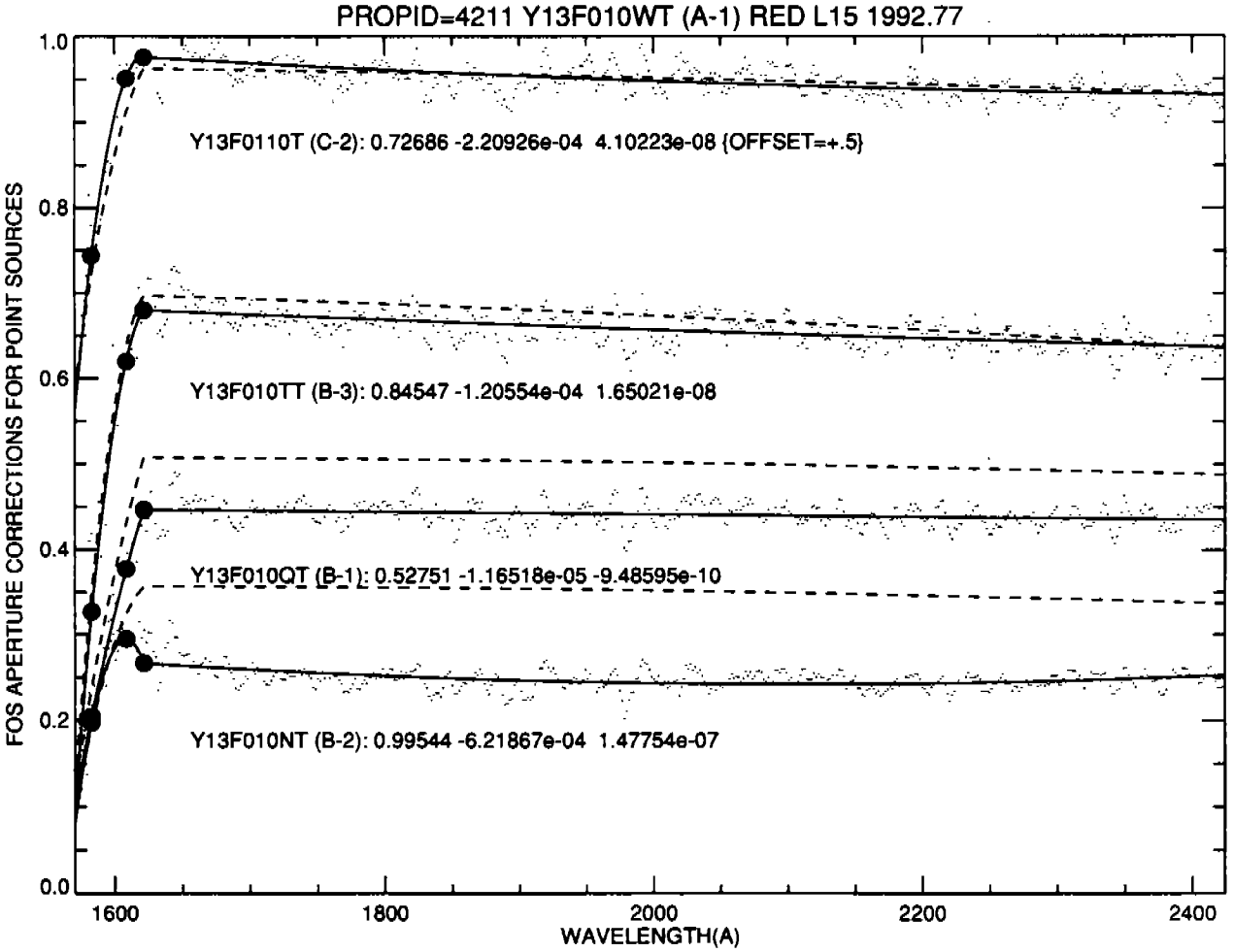
PROPID=4211 Y13F010WT (A-1) RED L15 1992.77
FOS APERTURE CORRECTIONS FOR POINT SOURCES
1.0
0.8
0.6
0.4
0.2
0.0
Y13F0110T (C-2): 0.72686 -2.20926e-04 4.10223e-08 {OFFSET=+.5}
Y13F010TT (B-3): 0.84547 -1.20554e-04 1.65021e-08
Y13F010QT (B-1): 0.52751 -1.16518e-05 -9.48595e-10
Y13F010NT (B-2): 0.99544 -6.21867e-04 1.47754e-07
1600
1800
2000
2200
2400
WAVELENGTH(A)

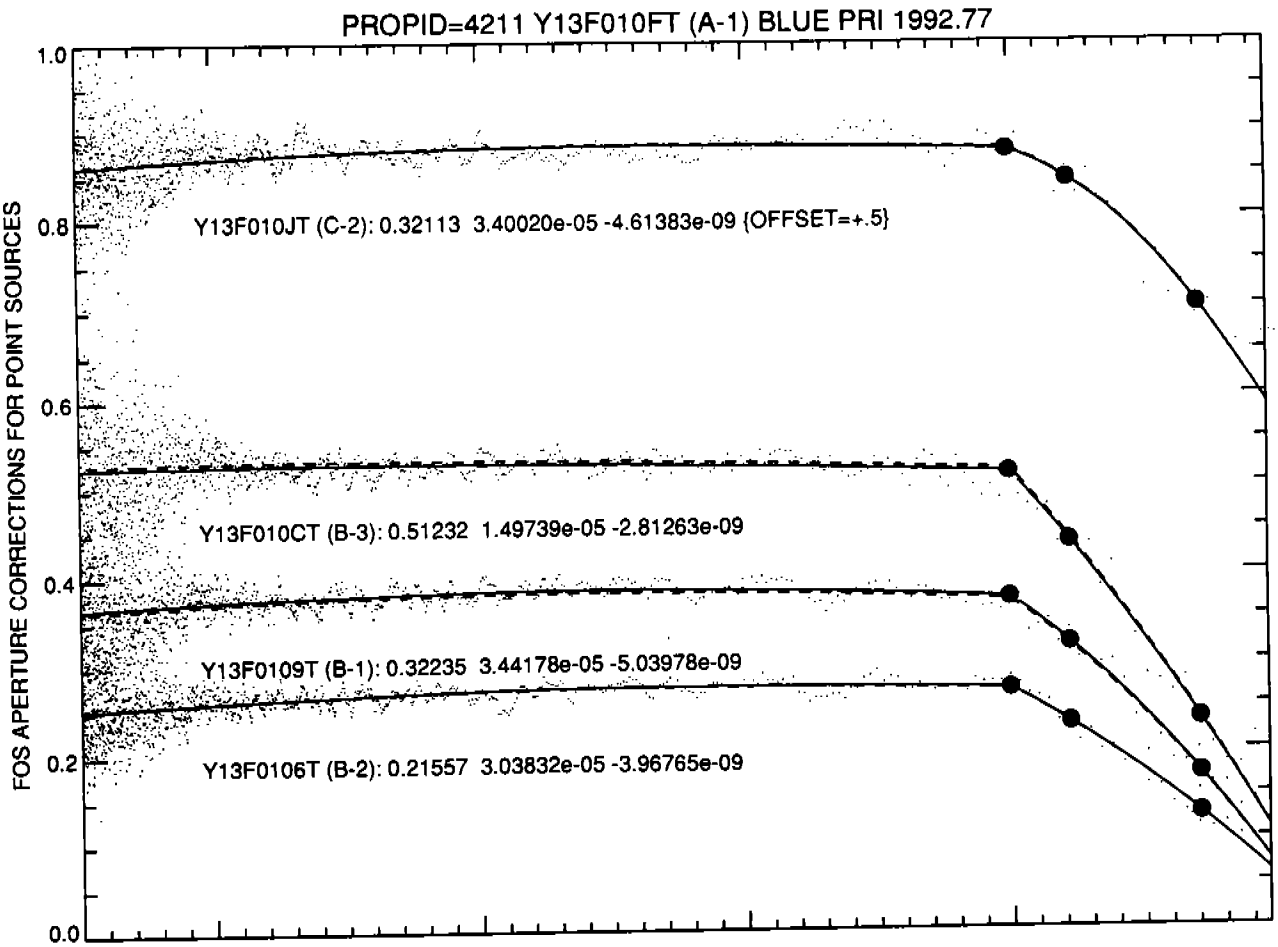
PROPID=4211 Y13F010FT (A-1) BLUE PRI 1992.77
FOS APERTURE CORRECTIONS FOR POINT SOURCES
1.0
0.8
0.6
0.4
0.2
0.0
Y13F010JT (C-2): 0.32113 3.40020e-05 -4.61383e-09 {OFFSET=+.5}
Y13F010CT (B-3): 0.51232 1.49739e-05 -2.81263e-09
Y13F0109T (B-1): 0.32235 3.44178e-05 -5.03978e-09
Y13F0106T (B-2): 0.21557 3.03832e-05 -3.96765e-09

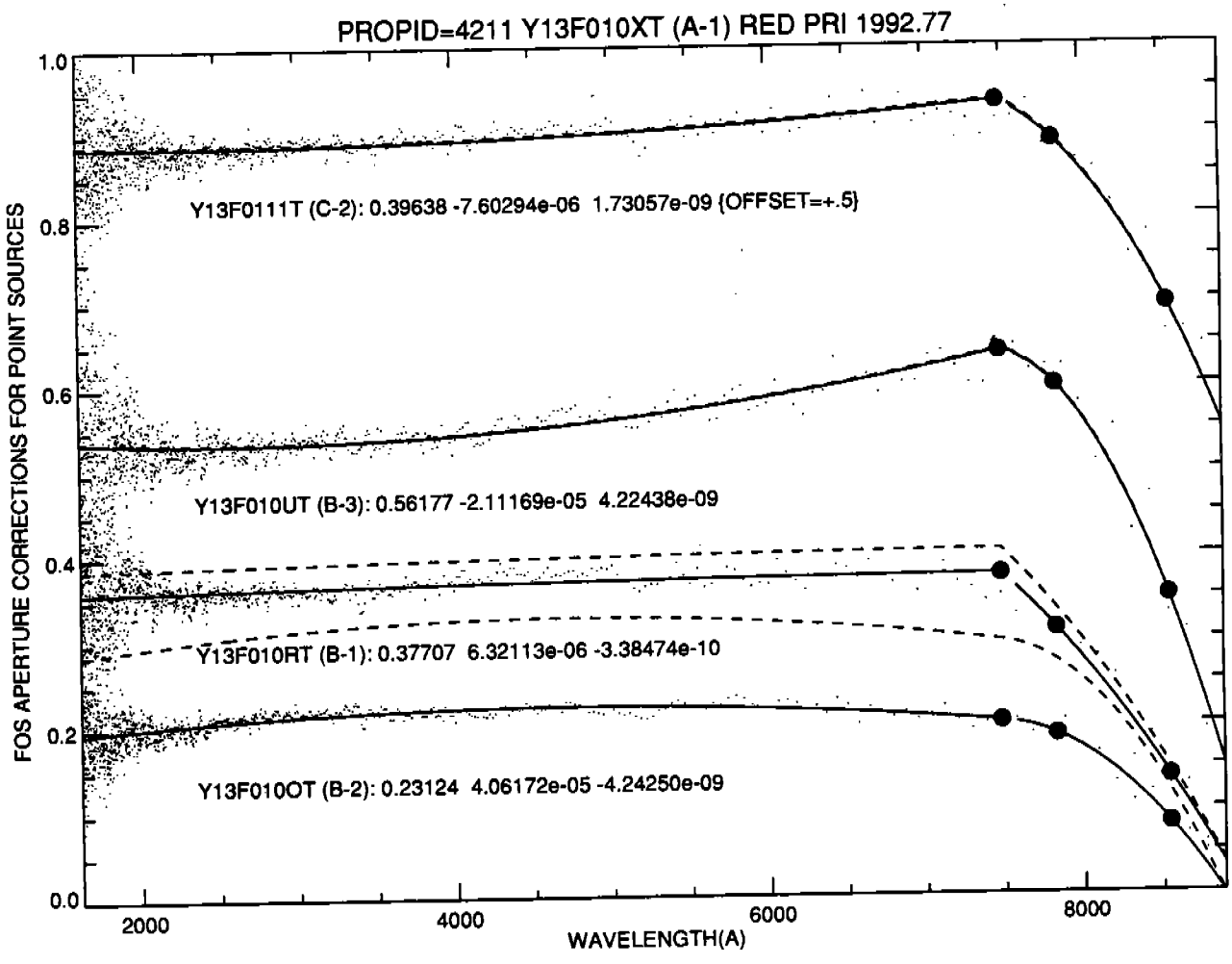
PROPID=4211 Y13F010XT (A-1) RED PRI 1992.77
FOS APERTURE CORRECTIONS FOR POINT SOURCES
1.0
0.8
0.6
0.4
0.2
0.0
Y13F0111T (C-2): 0.39638 -7.60294e-06 1.73057e-09 {OFFSET=+.5}
Y13F010UT (B-3): 0.56177 -2.11169e-05 4.22438e-09
Y13F010RT (B-1): 0.37707 6.32113e-06 -3.38474e-10
Y13F010OT (B-2): 0.23124 4.06172e-05 -4.24250e-09
2000
4000
6000
8000
WAVELENGTH(A)